

**EVALUATION OF PATIENT DOSE UNDERGOING COMMON
RADIOLOGIC EXAMINATIONS AT RAMATHIBODI
HOSPITAL USING IAEA TRS 457 PROTOCOL**

KRONVADEE PROMSUPAP

**A THESIS SUBMITTED IN PARTIAL FULFILLMENT
OF THE REQUIREMENTS FOR THE DEGREE OF
MASTER OF SCIENCE (MEDICAL PHYSICS)
FACULTY OF GRADUATE STUDIES
MAHIDOL UNIVERSITY
2012**

COPYRIGHT OF MAHIDOL UNIVERSITY

Thesis
entitled
**EVALUATION OF PATIENT DOSE UNDERGOING COMMON
RADIOLOGIC EXAMINATIONS AT RAMATHIBODI
HOSPITAL USING IAEA TRS 457 PROTOCOL**

.....
Miss Kronvadee Promsupap
Candidate

.....
Asst. Prof. Napapong Pongnapang,
Ph.D. (Radiology-Medical Physics)
Major advisor

.....
Lect. Puangpen Tangboonduangjit,
Ph.D. (Medical Radiation Physics)
Co-advisor

.....
Prof.Banchong Mahaisavariya,
M.D.,Dip Thai Board of Orthopedics
Dean
Faculty of Graduate Studies
Mahidol University

.....
Lect. Puangpen Tangboonduangjit,
Ph.D. (Medical Radiation Physics)
Program Director
Master of Science Program
in Medical Physics
Faculty of Medicine
Ramathibodi Hospital
Mahidol University

Thesis
entitled
**EVALUATION OF PATIENT DOSE UNDERGOING COMMON
RADIOLOGIC EXAMINATIONS AT RAMATHIBODI
HOSPITAL USING IAEA TRS 457 PROTOCOL**

was submitted to the Faculty of Graduate Studies, Mahidol University
for the degree of Master of Science (Medical Physics)

on
May 22, 2012

.....
Miss Kronvadee Promsupap
Candidate

.....
Assoc.Prof. Anchali Krisanachinda,
Ph.D. (Medical Radiation Physics)
Chair

.....
Asst.Prof. Napapong Pongnapang,
Ph.D. (Radiology-Medical Physics)
Member

.....
Lect. Puangpen Tangboonduangjit,
Ph.D. (Medical Radiation Physics)
Member

.....
Prof. Banchong Mahaisavariya,
M.D., Dip Thai Board of Orthopedics
Dean
Faculty of Graduate Studies
Mahidol University

.....
Prof. Winit Phuapradit,
M.D., M.P.H.
Dean
Faculty of Medicine
Ramathibodi Hospital
Mahidol University

ACKNOWLEDGEMENTS

The success of this thesis had been attributed to the extensive support and assistance from my major advisors, Asst.Prof. Napapong Pongnapang, my co-advisor Dr.Puangpen Tangboonduangjit and Asst.Prof. Sawwanee Asavaphatiboon (Department of Radiology, Faculty of Medicine, Ramathibodi hospital). I would like to express my deep gratitude and appreciation for their valuable advice, supervision, guidance, and encouragement throughout this research study.

I wish to thank Assoc.Prof. Anchali Krisanachinda (Department of Radiology, Faculty of Medicine, Chulalongkorn University) for her kindness in examining the research, providing suggestions for improvement, and acts the external examiner of the thesis defense.

I also wish to thank all staffs of Department of Radiology, Faculty of Medicine, Ramathibodi Hospital for their helpful support and kind co-operation during the entire experiment.

I am grateful to all the lecturers and all staffs in the School of Medical Physics at Division of Radiation Oncology and Nuclear Medicine, Ramathibodi Hospital for their kind support, understanding, encouragement and supply the academic knowledge on medical physics.

Finally, I am grateful to my family and all friends for their love, care and support thought this course of study.

Kronvadee Promsupap

EVALUATION OF PATIENT DOSE UNDERGOING COMMON RADIOLOGIC EXAMINATIONS AT RAMATHIBODI HOSPITAL USING IAEA TRS 457 PROTOCOL**KRONWADEE PROMSUPAP 5037330 RAMP/M****M. Sc. (MEDICAL PHYSICS)****THESIS ADVISORY COMMITTEE : NAPAPONG PONGNAPANG, Ph.D. (RADIOLOGY-MEDICAL PHYSICS), PUANGPEN TANGBOONDUANGJIT, Ph.D. (MEDICAL RADIATION PHYSICS)****ABSTRACT**

The objective of this study was to determine dosimetry for standard size Thai populations undergoing radiographic examination and fluoroscopy examinations at Ramathibodi hospital, based on the IAEA TRS 457 protocol. The goal was to establish diagnostic reference levels and to compare the values with the those reported by the International Atomic Energy Agency, the Commission of the European Community, United Kingdom, Malaysia and Ireland, respectively. This study includes data from the patients weight-ranged, from 52 -62 kg for female and 64-74 kg for male subjects, based on standard size data for Thai population published in <http://thailand.prd.go.th>.

For radiographic examinations, the patient dosimetry was determined in terms of the entrance surface air kerma on the basis of X-ray tube output measurements and exposure parameter by ionization chamber. The data from three digital radiography units in six digital radiographic examinations including skull AP, skull lateral, chest PA, abdomen AP, lumbar spine AP and lumbar spine lateral. The DRLs for skull AP, skull lateral, chest PA, abdomen AP, lumbar spine AP and lumbar spine lateral were 1.73, 1.33, 0.06, 4.05, 6.23 and 6.45 mGy, respectively.

For fluoroscopy examination, the patient dosimetry was determined in terms of the air kerma area product for upper GI, barium meal, and lower GI examination, barium enema, calculated by KAP meter reading combined with calibration coefficient of the reference dosimeter. The DRLs for barium meal was 12.53 cGy cm² and barium enema was 14.82 cGy cm².

The results showed that the DRLs for this study were less than the values established or surveyed by the other studies except skull lateral, lumbar spine AP and barium meal examinations. The lower DRLs found in this study resulted from the multifactor example image receptor technology exposure techniques and patient size. A CsI based a-Si TFT technology used in the digital system has better detection efficiency than conventional screen-film system. With proper exposure parameters, one can optimize image quality while maintaining the lowest possible radiation dose exposure for the patients.

**KEY WORDS: DIAGNOSTIC REFERENCE LEVELS/ DIGITAL RADIOGRA-
PHY/ ENTRANCE SURFACE AIR KERMA/ AIR KERMA
AREA PRODUCT**

54 pages

การประเมินปริมาณรังสีที่ผู้ป่วยได้รับจากการตรวจทางรังสีวินิจฉัยในโรงพยาบาลรามธิบดีโดยใช้ระเบียบการของทบวงการพลังงานปรมาณูระหว่างประเทศ TRS 457
(EVALUATION OF PATIENT DOSE UNDERGOING COMMON RADIOLOGIC EXAMINATIONS AT RAMATHIBODI HOSPITAL USING IAEA TRS 457 PROTOCOL)

กรวดี พรหมสุภาพ 5037330 RAMP/P

วท.ม. (ฟิสิกส์การแพทย์)

คณะกรรมการที่ปรึกษาวิทยานิพนธ์: นภาพงษ์ พงษ์นภางค์ Ph.D. (RADIOLOGY-MEDICAL PHYSICS), พวงเพ็ญ ตั้งบุญดวงจิตร, Ph.D. (MEDICAL RADIATION PHYSICS)

บทคัดย่อ

วัตถุประสงค์ของการศึกษานี้เพื่อประเมินปริมาณรังสีที่ผู้ป่วยได้รับจากการเอกซเรย์ทั่วไปและการส่องตรวจทางรังสีในโรงพยาบาลรามธิบดีโดยใช้ระเบียบการของทบวงการพลังงานปรมาณูระหว่างประเทศ TRS 457 เพื่อสร้างระดับปริมาณรังสีอ้างอิงและเปรียบเทียบกับค่าจากการศึกษาอื่นๆ เช่น ทบวงการพลังงานปรมาณูระหว่างประเทศ สมาคมยุโรป ประเทศสหรัฐอเมริกา มาเลเซียและไอร์แลนด์ ทำการศึกษาในคนไทยที่มีรูปร่างปกติคือผู้หญิงน้ำหนัก 52 ถึง 62 กิโลกรัมและผู้ชาย 54 ถึง 64 กิโลกรัม ในการตรวจเอกซเรย์ทั่วไป จำนวนปริมาณรังสีที่ผิวทางเข้า โดยใช้ค่าปริมาณรังสีจากหลอดเอกเรย์และพารามิเตอร์ สำหรับการถ่ายภาพเอกซเรย์กะโหลกศีรษะท่า AP และท่า Lat ปอด PA ช่องท้อง AP กระดูกสันหลัง AP และท่า Lat โดยเครื่องเอกซเรย์ระบบดิจิทัลสามเครื่อง พบว่าระดับปริมาณรังสีอ้างอิง มีค่าดังนี้ 1.73, 1.33, 0.06, 4.05, 6.23 และ 6.45 มิลลิเกรย์ ตามลำดับ การส่องตรวจทางรังสีใช้ปริมาณรังสี KAP สำหรับการตรวจทางเดินอาหารส่วนต้นและทางเดินอาหารส่วนปลาย พบว่าปริมาณรังสีอ้างอิงมีค่า 12.53 และ 14.82 เซนติเกรย์ตารางเซนติเมตรตามลำดับ จากผลการศึกษาสรุปได้ว่าปริมาณรังสีอ้างอิงที่ได้จากการศึกษานี้มีค่าน้อยกว่าค่าจากการศึกษาอื่น ยกเว้นในการถ่ายภาพเอกซเรย์กะโหลกศีรษะท่า Lat กระดูกสันหลังท่า AP และการตรวจทางเดินอาหารส่วนต้น เนื่องจากปัจจัยต่างๆ เช่น เทคโนโลยีตัวรับภาพ ค่าพารามิเตอร์ที่ใช้ในการถ่ายภาพและน้ำหนักของผู้ป่วย เป็นต้น

CONTENTS

	Page
ACKNOWLEDGEMENTS	iii
ABSTRACT (ENGLISH)	iv
ABSTRACT (THAI)	v
LIST OF TABLES	vii
LIST OF FIGURES	ix
LIST OF ABBREVIATIONS	xi
CHAPTER I INTRODUCTION	1
CHAPTER II OBJECTIVES	13
CHAPTER III LITERATURE REVIEW	14
CHAPTER IV MATERIALS AND METHODS	18
CHAPTER V RESULTS	27
CHAPTER VI DISCUSSION	42
CHAPTER VII CONCLUSION	46
REFERENCES	47
APPENDIX	50
BIOGRAPHY	54

LIST OF TABLES

Table	Page
1.1 The radiation weighting factor for the various types of radiation and energies.	8
1.2 The tissue weighting factor for the various types of tissue or Organ.	10
1.3 Threshold dose for deterministic effect.	12
2.1 The Entrance surface dose for seven routine X-ray examinations from a random sample of 12 hospitals in Malaysia.	14
5.1 The HVL of digital radiography in X ray room no.6 for varies tube voltage.	28
5.2 The tube output of digital radiography in X ray room no.6.	30
5.3 The tube output of digital radiography in X ray room no.8 for field size 30×30 cm ² .	30
5.4 The tube output of digital radiography in X ray room no.8 for field size 40×40 cm ² .	31
5.5 The tube output of digital radiography in X ray room no.8 for field size 43×43 cm ² .	31
5.6 The tube output of digital radiography in X ray room no.9 for field size 35×35 cm ² .	32
5.7 The tube output of digital radiography in X ray room no.9 for field size 35×43 cm ² .	32
5.8 The mean patient information and exposure parameters for six common radiographic examinations.	34

LIST OF TABLES (cont.)

Table	Page
5.9 The mean, median, third quartile values, minimum, maximum entrance surface air kerma in mGy, standard deviation, inter-quartile range and ratio of maximum/minimum for each examination.	34
5.10 A Comparison diagnostic reference levels of entrance surface air kerma in mGy for each examination.	35
5.11 The calibration coefficient of KAP meter in digital fluoroscopy.	38
5.12 The mean patient characteristic and exposure parameters for barium meal and barium enema examinations.	40
5.13 Air kerma area products in cGy cm^2 for barium meal and barium enema examinations.	41
5.14 A Comparison diagnostic reference levels of Air kerma area product in cGy cm^2 for barium meal and barium enema examination.	41
A-1 The backscatter factor for water, ICRU tissue and PMMA for 21 diagnostic x ray beam qualities and for three field sizes at a focus to skin distance of 1000 mm.	51

LIST OF FIGURES

Figure	Page
1.1 Direct readout electronic x-ray detectors use either a direct technique or an indirect technique for converting x-ray into an electric charge.	3
1.2 The image intensifier composition.	5
1.3 The radiation weighting factor for various neutrons energies.	9
1.4 The relationship between radiation doses with severity for deterministic and stochastic effect.	12
4.1 Digital radiography machine.	18
4.2 Digital fluoroscopy machine.	19
4.3 Accu-Pro™ Diagnostic Ion Chamber and kV Sensor Components	20
5.1 The HVL of varies tube voltage for digital radiography in X ray room no.6.	28
5.2 The tube output as a function of varies tube voltage and tube loading for digital radiography in X ray room no.8.	29
5.3 The tube output as a function of varies tube loading and 109 kVp tube voltage for digital radiography in X ray room no.9.	33
5.4 Comparison diagnostic reference level of entrance surface dose.	36
5.5 The calibration coefficient as a function of varies tube voltage for digital fluoroscopy.	38
5.6 The correlation of the air kerma area products versus fluoroscopy time (left) and air kerma area products versus number of image (right) for barium meal examination.	40
5.7 The correlation of the air kerma area products versus fluoroscopy time (left) and air kerma area products versus number of image (right) for barium enema examination.	40

LIST OF ABBREVIATIONS

Abbreviations	Term
AEC	Automatic exposure control
AgBr	Silver bromide
AgI	Silver iodide
Al	Aluminium
AP	Anteroposterior
B	Backscatter factor
BaFBr	Barium fluorobromide
BaFI	Barium fluoroIodide
CaWO ₄	Calcium tungstate
CCD	Charged coupled device
CEC	Commission of the European Community
cGycm ²	centigray squarecentimeter
CR	computed radiography
CsI	Cesium iodide
d	distance
DAP	Dose area product
DRL	Diagnostic reference levels
D _T	Mean absorbed dose in a specified tissue or organ
EAK	Entrance air kerma
FFD	X-ray tube focus-film distance
FSD	X-ray tube focus-skin distance
Gy	Gray
IAEA	International Atomic Energy Agency
KAP	Air kerma area product
K _e	Entrance surface air kerma

LIST OF ABBREVIATIONS (cont.)

Abbreviations	Term
K_i	Incident air kerma
kVp	Kilo voltage peak
LAT	Lateral
LET	Linear energy transfer
mA	milliampere
man Sv	man sievert
NRPB	National Radiological Protection Board
PA	Posteroanterior
P_{It}	Tube current exposure time product
P_{KA}	Air kerma area product
QC	Quality control
Si	Silicon
TFT	Thin film transistor
TLD	Thermoluminescent Dosimeter
UK	United kingdom
UNSCEAR	United Nation Scientific Committee on the Effect of Atomic Radiation
W_R	Radiation weighting factor
W_T	Tissue weighting factor
X_{air}	Exposure in air
$Y_{(d)}$	Tube output
ZnCdS:Ag	Zinc cadmium sulfide doped with silver

CHAPTER I

INTRODUCTION

In 1895, Wilhelm Conrad Roentgen discovered X-rays. Since then, the use of X-rays has contributed to the medicine. Medical image systems have developed from simple units to systems that can visualize the whole body, obtain information concerning functional aspects specific organs and even yield information about the chemistry taking place in organs and tissues.

Digital radiography has been introduced to the Thai healthcare service for more than 10 years. It has been gradually replacing conventional screen-film radiography. The advantages for digital radiography over conventional radiography are greater dynamic range, wider exposure latitude, instant display image, post processing image available, easily transmitted image through network and archive. The development technology of detector in general radiography and fluoroscopy were described.

1.1 Modality

1.1.1 General radiography

General radiography has been established for the first medical image technology. It consists of an X-ray source on one side of the patient, and an X-ray detector on the other side. The homogeneous distributions of X-ray are emitted by the X-ray tube and attenuated in the patient. The attenuation is depended on the type and the thickness of the tissue which they pass. The heterogeneous distribution of X-rays are emerged from the patient and exposed to the detector. The radiographic image is established from this X-ray distribution. The detectors used are the screen-film system or digital system.

1.1.1.1 The screen-film system

The screen film system consists of a cassette, intensifying screen and sheet of film. The front surface of the X-ray cassette is designed for maximize the transmission of the X-rays which usually made of carbon fiber. Intensifying screen is made of scintillating material or phosphor which calcium tungstate (CaWO_4) has been used for the most common scintillator material. X-ray energy is converted by scintillator material into light and then it is striked to the film. Film is made from one or two layers of film emulsion coated onto a flexible sheet or Mylar. The film emulsion is made from the grains of silver halide (AgBr and AgI) bound in a gelatin base (1).

1.1.1.2 The computed radiography

Computed radiography was introduced in the 1970s. It have been gradually replaced screen film system and converted analog to digital system. The CR image plate are made of barium fluorohalide material which consist of 85% BaFBr and 15% BaFI activated with a small quantity of europium. The electrons associated with the europium atoms are excited, when the X-ray energy was absorbed by the BaFBr phosphor. The divalent europium atom is oxidized and changed to the trivalent state. The excited electrons are become mobile and some fractions of them are interacted with F-center. These electrons are trapped in metastable state of F-center and developed to the latent image. The number of trapped electron per unit area of the imaging plate is proportion to the intensity of X-rays incident at each location during the exposure.

The digital images are developed from the latent image by readout process. The exposed imaging plate is scanned by the red laser light and these light are absorbed by the F-center. The energy of the red laser light is transferred to the electrons. Blue-green lights are released when these electrons have energy enough to the conduction band. These electrons are become de-excited and reabsorbed by the trivalent europium atoms. The divalent europium atom is converted. Then, the image plate is exposed by very bright light source for erase the latent image and it can be reused for another exposure without ghosting. The advantages of CR over screen-film

system are reduce repeat expose due to overexposure or underexposure and had larger dynamic range (1).

1.1.1.3 The digital radiography

The digital radiography is direct-readout digital detectors which have been used since the introduction of the charged-coupled device (CCD) but continuous development in technology will be made possible a new generation of detector. The detector for digital radiography can be divided into two types are direct methods which converted X-ray into an electric charge such as amorphous selenium and indirect methods which converted X-ray into visible light and that light is then converted into an electric charges such as amorphous silicon photodiode arrays or CCDs. However, the electric charges are sent to an electronic readout mechanism and analog to digital conversion for direct and indirect conversion detectors to produce the digital image (1, 2).

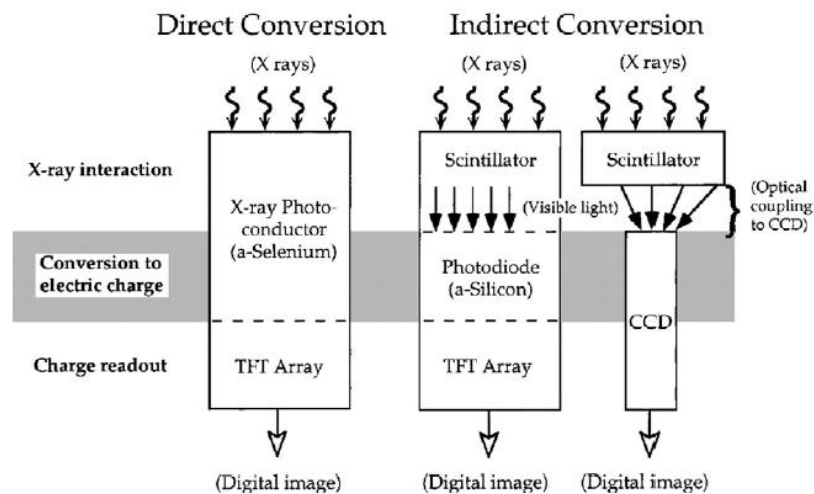


Figure 1.1 Direct readout electronic X-ray detectors use either a direct technique or an indirect technique for converting X-ray into an electric charge (2).

i. The Charged Coupled Devices (CCD). The Charged Coupled Devices (CCD) is consisted of a series of metal-oxide- semiconductor capacitors manufactured very close together on a semiconductor surface.(see figure 1.1) They are used in a wide variety of indirect conversion X-ray imaging devices. The physical

characteristic of CCDs in digital radiography typically 2-4 cm² is smaller than projected X-ray areas. Therefore the sizes of the projected visible light image from a scintillator are reduced and transferred to the face of one or more CCDs by the optical coupling device. The optical coupling device can be used the optical lens system or the fiberoptic taper. The numbers of photons into the CCDs are reduced by the optical lens system for reduce the appearance of image noise, geometric distortions, optical scatter and increase spatial resolutions which improve image quality. Reduction light loss and optical scatter are performed by the fiberoptic tapers but structure artifacts on the image will be introduced from imperfections in the optical fiber bundles.

ii. Indirect conversion detectors. The top layers of the thin film transistor sandwich are contacted with the amorphous silicon photodiode circuit and scintillator. Thin film transistor arrays are typically deposited onto a glass substrate in multiple layers. When the scintillator is exposed by X-ray, visible light photons are emitted proportional to the incident X-ray energy. Then, they are converted into electric charges by the photodiode array. Finally, the electronic charges are collected at each photodiode and converted into a digital value by using the underlying readout electronics.

iii. Direct conversion detectors. The amorphous selenium is used as the photoconductor material because of its excellent X-ray detection properties and a high intrinsic spatial resolution. They are placed on the top layer of the electronic thin film transistor sandwich. Before exposure, an electric field is applied across the amorphous selenium layer through a bias electrode on the top surface of the selenium. When X-rays are absorbed in the detector, electrons and holes are released within the selenium. The electric charges are drawn directly to the charge-collecting electrodes owing to the electric field within the selenium.

1.1.2 Fluoroscopy

Fluoroscopy is real time radiography which a sequence of X-ray image is continuous acquired. It is used for visualizing contrast agents in the gastro-intestinal tract and other medical application such as invasive procedures where real-time image feedback is necessary (1).

Fluoroscopy systems are consisted of major components following;

1. The X-ray tube typically use between 50-110 kVp. The tube voltage and tube current was set to required contrast and lowest possible dose for patient.

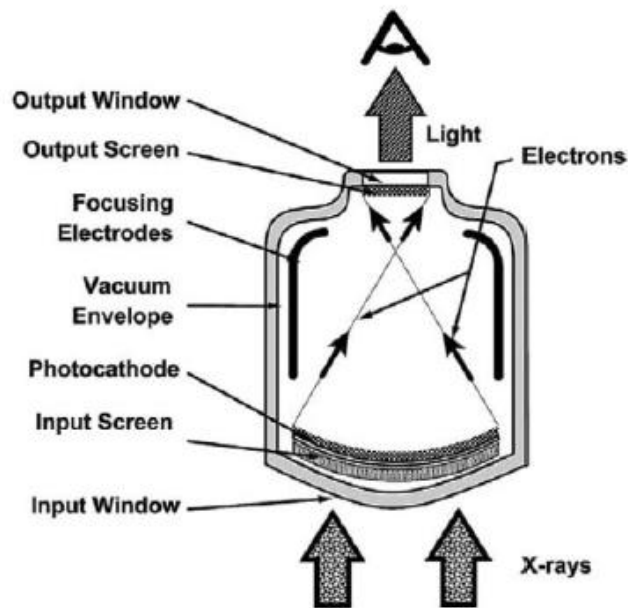


Figure 1.2 The image intensifier composition (3).

2. The image intensifier are consist of (see figure 1.2) input fluorescent screen, photocathode and output fluorescent screen. Input fluorescent screen is composed of four layers. First and second layers are made of Al for keep the air out of II, support input phosphor and photocathode layers, respectively. The input phosphor is made of CsI crystal for convert X-ray photon to light photon. Finally, photocathode layer is made of a metal compound for convert light photon to electrons. The electrons from the photocathode are controlled by electronic lens for focus onto the output phosphor. When electrons incident, the light photons approximately 1000 are emitted from the output phosphor The output fluorescent screen is made of zinc cadmium sulfide doped with silver (ZnCdS:Ag).

3. The output image of the II is coupled with image receptor example video camera, TV monitor and film by the optical system. The signal from output of the II is transferred to the video monitor by the video camera system.

4. The brightness of the image is kept constant for the monitor by the AEC system which regulated the exposure rate of X-ray for incident on the input phosphor of the II.

Flat panel devices are thin film transistor array that are rectangular in format and are used as X-ray detectors. TFT systems are pixilated devices with a photodiode at each detector element, which converts light energy to an electronic signal. Since the TFT array is sensitive to visible light (and is not very sensitive to X-ray), a scintillator such as CsI is used to convert the incident X-ray beam energy into light, which then strikes the TFT detector. The pixel size in fluoroscopy is usually larger than radiography, and some flat panel systems have the ability to adjust the pixel size by binning four pixels into one larger pixel. Such dual-use systems have pixels small enough to be adequate for radiography, but the pixels can be binned to provide a detector useful for fluoroscopy. Flat panel imagers can therefore lighter and smaller package. Because a vacuum environment is not required, the cover to the flat panel can be about 1 mm of carbon fiber, and this improves the quantum detection efficiency compared to the image intensifier (1,2).

1.2 Dosimetry

International organization, regulatory bodies and standard organization have been interesting radiation dose to patients during diagnostic examination. In 2008, the report of the United Nation Scientific Committee on the Effect of Atomic Radiation (UNSCEAR) indicated that the frequency of diagnostic examination have increased from 1970-1979 especially in health-care level II countries is 12.7 times in 1997-2007. The total annual collective effective dose to global population from diagnostic examination is 4,000,000 manSv increasing from previous study approximately 1,700,000 manSv, which 25% received from health-care level II countries. According this report, the annual collective dose increases because of the increasing of the frequency of diagnostic examination, effective dose per examination (from 0.4 mSv to 0.62 mSv) and the global population (from 5,800 million to 6,446 million) (4).

Patient dose in radiologic examination has been reported by various national and international dose surveys. The wide variation in patient dose for the same type of radiographic examination was observed due to the differences in exposure parameters and the equipment used. Therefore the hospital should establish own dose reference levels and compare with reliability organization in order to assess appropriate of examination procedure and optimize patient protection.

1.2.1 Dosimetric Quantities

Dosimetric Quantities are used for measurements radiation dose on patient in this study generally follows ICRU 74 (5, 6, 7).

1.2.1.1 Incident air kerma.

The incident air kerma (K_i) is the kerma to air which measurement on patient or phantom surface at central beam axis from an incident X-ray beam and exclude backscatter radiation. The name for the unit of kerma is gray.

1.2.1.2 Entrance surface air kerma.

The entrance surface air kerma (K_e) is the kerma to air which measurement on patient or phantom surface at central beam axis from an incident X-ray beam and include backscatter radiation. The entrance surface air kerma is product of incident air kerma with backscatter factor (B) thus.

$$K_e = K_i B$$

The name for the unit of kerma is gray (Gy).

1.2.1.3 X-ray tube output.

The X-ray tube output ($Y(d)$) is the quotient of the air kerma at a specified distance (d) from the X-ray tube focus by the tube current–exposure time product (P_{It}) thus:

$$Y(d) = K(d) / P_{It}$$

Unit: $J \cdot kg^{-1} \cdot C^{-1}$. If the special name gray is used, the unit of X-ray output is Gy/C.

1.2.1.4 Air kerma–area product.

The air kerma–area product, P_{KA} , is the integral of the air kerma over the area of the X-ray beam in a plane perpendicular to the beam axis thus:

$$P_{KA} = \int_A K(x,y) dx dy$$

Unit: $J \cdot kg^{-1} \cdot m^2$. If the special name gray is used, the unit of air kerma–area product is $Gy \cdot m^2$.

The air kerma area product has the useful property that it is approximately invariant with distance from the X-ray tube focus (when interactions in air and extrafocal radiation can be neglected) when as long as the planes of measurement and calculation are not so close to the patient or phantom that there is a significant contribution from backscattered radiation.

Table 1.1 The radiation weighting factor for the various types of radiation and energies (6).

Radiation type	Radiation weighting factor (W_R)
Photon, all energies	1
Electrons, myons, all energies	1
Protons and charged pions	2
Alpha particles, fission fragments, heavy ions	20
Neutrons	A continuous function of neutron energy (see figure 4)

1.2.1.5 Organ and tissue dose.

The organ and tissue dose (D_T) is the mean absorbed dose in a specified tissue or organ. It is equal to the ratio of the energy imparted to the tissue or organ to the mass of the tissue or organ.

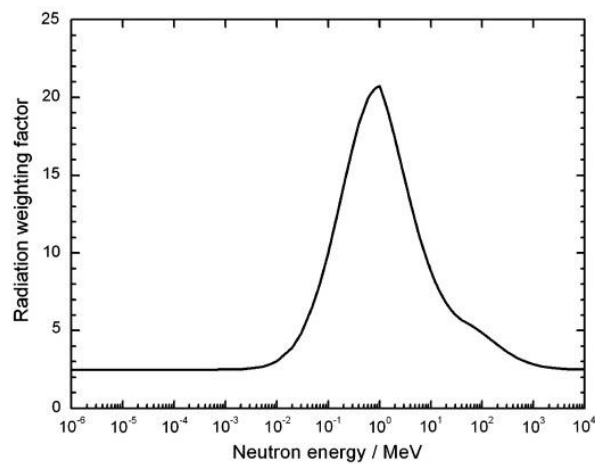
$$D_T = \frac{\epsilon_T}{m_T}$$

1.2.1.6 Equivalent dose.

The equivalent dose is the product of organ dose with radiation weighting factor. Owing to, the same organ dose was delivered by different types of radiation may result in different degree of biological damage to tissue. Therefore, the type of radiation being absorbed was considered for the harmful biological effects. Thus,

$$H_T = D_T \times w_R$$

w_R is radiation weighting factor which it is directly related to the LET of the radiation. The linear energy transfer (LET) is linear rate of energy loss of charged particle radiation in a medium. The radiation with a high LET is more damage to tissue than a low LET. The radiation weighting factor for various radiations are shown in the table 1.1 and figure 1.3



$$w_R = \begin{cases} 2.5 + 18.2e^{-[\ln(E_n)]^2/6}, & E_n < 1 \text{ MeV} \\ 5.0 + 17.0e^{-[\ln(2E_n)]^2/6}, & 1 \text{ MeV} \leq E_n \leq 50 \text{ MeV} \\ 2.5 + 3.25e^{-[\ln(0.04E_n)]^2/6}, & E_n > 50 \text{ MeV} \end{cases}$$

Figure 1.3 The radiation weighting factor for various neutrons energies (6).

1.2.1.7 Effective dose.

The effective dose is the sum individual tissue dose value multiplied by the tissue weighting factor. The different sensitivity of tissue was existed for the occurrence of stochastic radiation effects. This different was concerned by the tissue weighting factor following equation.

$$E = \sum_T w_T \times H_T$$

w_T is tissue weighting factor which the tissue weighting factor for various tissue are shown in the table 1.2

Table 1.2 The tissue weighting factor for the various types of tissue or organ (8).

Tissue	W_T	ΣW_T
Bone-marrow(red), Colon, Lung, Stomach, Breast, Remainder tissues*	0.12	0.72
Gonads	0.08	0.08
Bladder, Esophagus, Liver, Thyroid	0.04	0.16
Bone surface, Brain, Salivary glands, Skin	0.01	0.04
	Total	1.00

* Remainder tissue: Adrenals, Extrathoracic (ET) region, Gall bladder, Heart, Kidneys, Lymphatic nodes, Muscle, Oral mucosa, Pancreas, Prostate, Small intestine, Spleen, Thymus, Uterus/cervix

1.2.1.8 Diagnostic Reference levels.

The diagnostic reference levels is dose level in medical diagnostic practices or in the case of radiopharmaceuticals, level of activity, for typical examinations for groups of standard-sized patients or standard phantoms for broadly defined types of equipment. These levels are expected not to be exceeded for standard procedures when good and normal practice regarding diagnostic and technical performance is applied.

1.2.2 Radiation effecting to patient.

Radiation is energy that it is emitted from sources including heat and light from the sun, microwaves from an oven, or X-rays from an X-ray tube. The characteristics of the radiation depend on its energy. Ionization refers to the process which the radiation has sufficient energy to remove an electron from an atom (e.g.,

gamma rays, X-rays) to form a pair of charged particles (i.e., ions). Lower energy radiation (e.g., radio waves, visible light) has insufficient energy to cause ionization. The resulting ions can be very destructive to biological material because they can break chemical bonds. Two types of cell damage occur; the cell can die or be damaged. In the event of cell death, the damage to the overall organism will only be significant if a sufficient number of cells are killed. Cell death will occur with a sufficient dose. Cell damage is more complicated. The cell may simply become nonviable and eventually die. Alternatively, the damage to the genetic code may be repaired. In the event that the repair is flawed and the cell remains viable, then mutations may result, eventually manifesting as cancer many years later. Carcinogenesis may or may not occur (9).

Ionizing radiation passing through living matter produces physical and chemical changes at various levels: molecular, cellular, tissue, and the whole organism. The chemicals and drugs are metabolized and transported through the placenta to the conceptus. Thus ionizing radiation affects the conceptus directly. Two types of effects can be produced by ionizing radiation: deterministic effects and stochastic effects.

1.2.2.1. Deterministic Effect.

Deterministic effects are caused by cell killing. These effects absolutely occur when tissue or organ received dose above a threshold dose. Below this threshold, the effects in exposed populations are similar to control populations who have received only background radiation. The severity of the effect increases respect to dose above the threshold dose as shown in figure 1.4. Cell killing can produce death; growth retardation; abnormal brain/central nervous system (CNS) development, including mental retardation and behavioral disorders; abortion; malformation; and cataracts. Threshold dose for deterministic effect are shown in the table 1.3.

1.2.2.2. Stochastic Effect.

Stochastic effects can occur after any exposure and involve damage to the nuclear material in cells are caused hereditary mutations or radiation

induced cancer including leukemia. There are no threshold doses which the chance of these effects increases with radiation dose, as shown in figure 1.4.

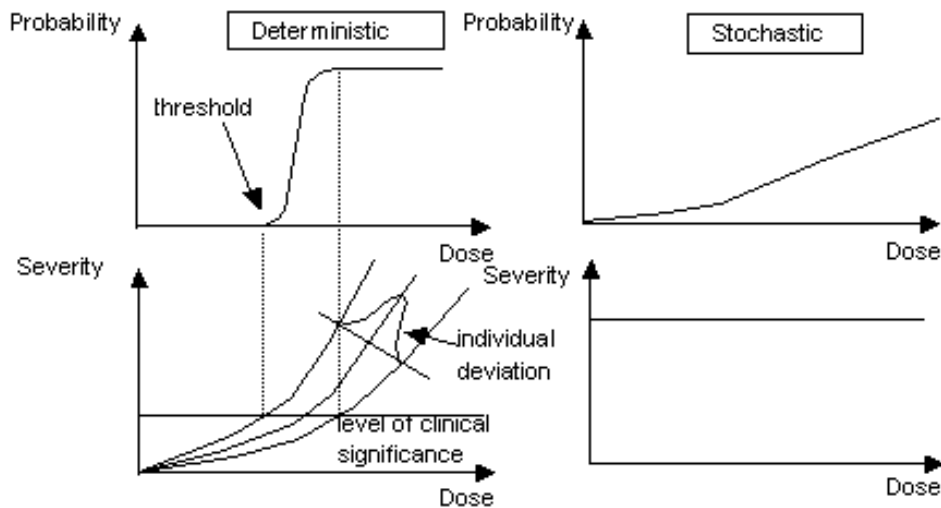


Figure 1.4 The relationship between radiation doses with severity for deterministic and stochastic effect.

Table 1.3 Threshold dose for deterministic effect (8).

Threshold for deterministic effects (Sv)			
	Effects	One single absorption (Sv)	Prolong absorption (Sv-year)
Testis	Permanent infertility	3.5 – 6.0	2
	Permanent infertility	2.5 – 6.0	> 0.2
Lens of eyes	Milky of lens	0.5 – 6.0	> 0.1
	cataract	5.0	> 0.15
Bone marrow	Blood forming deficiency	0.5	> 0.4

CHAPTER II

OBJECTIVE

The objective of this study was to establish diagnostic reference levels for general radiography and fluoroscopy examinations and to compare them with the diagnostic reference levels report by the International Atomic Energy Agency, the Commission of the European Community, United Kingdom, Malaysia, Ireland and other study. The patient dose was evaluated in standard size of Thai population at Ramathibodi Hospital based on IAEA TRS 457 protocol. Doses from common general radiographic examinations; skull AP, skull lateral, chest PA, abdomen AP, lumbar spine AP and lumbar spine lateral, fluoroscopic examinations; barium meal and barium enema were evaluated in this study.

The specific aims of this study are

1. To evaluate patient doses for general radiography and fluoroscopy examinations at Ramathibodi Hospital based on International Atomic Energy Agency Technical Reports Series no. 457 protocol.
2. To establish Diagnostic reference levels for general radiography and fluoroscopy examinations at Ramathibodi Hospital.
3. To compare Diagnostic reference levels from this study with by the International Atomic Energy Agency, the Commission of the European Community, United Kingdom, Malaysia, Ireland and other study.

CHAPTER III

LITERATURE REVIEWS

This study was performed to evaluate entrance surface air kerma (K_e) for general radiography examination and air kerma area product for fluoroscopy examination and to compare with the diagnostic reference levels reported by the International Atomic Energy Agency, the Commission of the European Community, United Kingdom, Malaysia, Ireland and other study. There are many authors reported the measurement of patient dose as described in the following;

In 1998, Ng Kwan Hoong et al. (10) established patient dose data with a mean weight around 60 kg within a range 45-75 kg from 1993-1995 in 12 randomly selected Malaysian public hospitals. Thermoluminescent dosimeter chips (TLD-100 Harshaw) were attached to the patient's skin at center of beam during examination which seven routine types (12 projections) were studied.

Table 2.1 The Entrance surface dose for seven routine X-ray examinations from a random sample of 12 hospitals in Malaysia .

Radiograph	Projection	Number	Entrance surface dose (mGy)					
			Min.	First quartile	Median	Mean	Third quartile	Max.
Chest	PA	131	0.05	0.16	0.26	0.28	0.35	0.74
	LAT	62	0.27	0.70	1.17	1.40	2.00	3.80
Abdomen	AP	99	1.67	5.98	9.22	10.00	13.82	24.45
Pelvis/hip	AP	70	1.14	3.81	5.33	8.41	11.08	30.91
Skull	AP/PA	103	0.72	3.11	4.74	4.78	6.85	8.27
	LAT	78	0.42	1.91	3.03	3.34	4.81	7.66
Cervical spine	AP	48	0.37	0.55	0.70	1.02	1.06	3.07
	LAT	46	0.23	0.60	1.49	1.60	2.28	3.96
Thoracic spine	AP/PA	22	2.21	4.79	6.39	7.03	8.72	12.87
	LAT	23	2.66	8.77	15.92	16.54	21.90	39.24
Lumbar spine	AP	88	2.24	5.34	9.06	10.56	14.71	30.68
	LAT	97	4.96	8.99	13.97	18.60	25.12	56.92

The result showed in table 2.1 for Entrance surface dose from a random sample of 12 hospitals in Malaysia. The table showed median ESD for chest PA, Chest lateral, abdomen AP, pelvis/hip AP, skull AP/PA, skull lateral, cervical spine AP, cervical spine lateral, thoracic spine AP, thoracic spine lateral, lumbar spine AP, lumbar spine lateral were 0.25, 1.17, 9.22, 5.33, 4.74, 3.03, 0.70, 1.49, 6.39, 15.92, 9.06 and 13.97 mGy, respectively. The median ESD values for all the projections are below the IAEA reference dose level, except cervical spine.

The study showed third quartile ESD value for chest PA, chest lateral, abdomen AP, pelvis/hip AP, skull AP/PA, skull lateral, cervical spine AP, cervical spine lateral, thoracic spine AP, thoracic spine lateral, lumbar spine AP, lumbar spine lateral of 0.35, 2.00, 13.82, 11.38, 6.85, 4.81, 1.06, 2.28, 8.72, 21.90, 14.71 and 25.12 mGy, respectively.

In 2000 Johnston and Brennan (11) established a baseline for the national reference dose levels in Ireland for chest, abdomen, pelvis and lumbar spine. Total of sixteen hospitals were chosen randomly and information of each hospital were collected on generator, tube, grid, automatic exposure control device, tabletop, film-screen type and speed, and type of quality assurance program. Lithium borate thermoluminescent dosimeters (TLDs) were placed on the entrance surface of patient at the center of X-ray beam during exposure and dose were read by the NRBP using a Toledo 654 TLD reader. Each hospital measured on 10 adult patients weighting within ± 13 kg of 70 kg for each projection except the lumbar sacral joint projection was examined in some hospitals less than 10 patients within the 6 weeks time period. Results showed reference dose level for chest PA, abdomen AP, pelvis AP, lumbar spine AP, lumbar spine LAT and lumbar sacral junction of 0.3, 6, 7, 8, 24 and 46 mGy, respectively. Reference dose levels were received from this study were less than UK data (1992), except the lumbar sacral joint projection and chest PA, which the lumbar sacral joint projection has higher while the chest PA projection has equal dose.

Retrospective patient dose analysis of a digital radiography system in routine clinical use was studied by Schuncke and Neitzel in 2005 (12). The KAP and EAK values were obtained from flat panel detector based digital radiography systems (Philips Digital Diagnost) at eleven hospitals, of which four are located in Germany, three other sites in Europe and four are located outside Europe. The study examined

doses for pelvis AP, lumbar spine AP, lumbar spine lateral, skull AP/PA, skull lateral, chest PA and chest lateral. The KAP and EAK values were compared with DRL for radiographic examination of adult patient in Germany. The Log file data for each image was generated automatically and comprised of identification data, examination data and dose data. The dose data showed KAP, detector dose and exposure indicator which EAK was obtained by KAP divided by the irradiation area in the patient entrance plane. The results showed median KAP and median EAK for all examination less than DRL in Germany and were founded wide variation at different hospitals. Multifactor had been influenced, for example sensitivity adjustment, parameter setting and patient. The Diagnostic reference levels refer to standard patient of 70 ± 10 kg but this study had no demographic information (age, sex, weight and size) therefore dose value was not correlated with patient size. Digital radiography systems have wide dynamic range and possibilities of flexible sensitivity adjustment. Thus dose monitoring is useful and necessary

In 2006, Kim et al. (13) estimated patient dose for simple radiographic examination, barium meal procedure and computed tomography in 32 hospitals in Korea. Ionization chamber (Rad/Cal corporation, model 20X5-60E) was used to measure in adult patients with a mean weight of 70 kg.

For radiographic examinations, the entrance surface doses (ESD) were derived from exposure in air (X_{air}) multiplied by backscatter factor. Ionization chamber was placed in air at the same distance to focus-skin distance and was exposed with exposure parameter used in each hospital. Results showed third quartile value for skull AP, skull lateral, chest PA, chest lateral, cervical spine AP, cervical spine lateral, thoracic spine AP, thoracic spine lateral, lumbar spine AP, lumbar spine lateral, shoulder AP, wrist, elbow, abdomen, hip AP, hip lateral, knee AP, pelvis AP, chest PA for children 4-6 years and chest AP for children 0-3 years of 2.76, 1.78, 0.28, 1.61, 1.44, 0.57, 2.85, 8.85, 3.56, 11.45, 0.77, 0.12, 0.19, 2.87, 2.9, 4.14, 0.51, 3.06, 0.26 and 0.24 mGy, respectively. The data showed doses from all projection were less than the IAEA reference levels and data form NRBP 2000.

For fluoroscopy, the dose area products (DAP) were determined for gastrointestinal study and barium enema study. The transmission ion chamber was calibrated against a reference dosimeter (Rad/Cal corporation, model 20X5-60E)

according to the National Radiological Protection Board (NRPB) protocol before measured DAP. Automatic mode was used for fluoroscopic tube potential, tube current and automatic brightness control during examination. Results showed that third quartile values for gastrointestinal study and barium enema study were 60.80 and 95.40 Gy·cm², respectively which were higher than the IAEA reference levels.

In 2003, Carroll and Brennan (14) established diagnostic reference levels (DRLs) for barium meal and barium enema examination in Ireland. Twelve hospitals were selected. The UK National Protocol for Patient Dose Measurements in Diagnostic Radiology was used for this study. The sample minimum of 10 adult patients per examination per hospital and mean weight lies within ± 5 kg of 70 kg was recommended. A DAP meter (VacuDAP 2001, J M Dolan & Co. Ltd, Dun Laoghaire, Dublin) was installed to measure dose area products in some hospitals without DAP meter. DAP was calibrated before any measurement recorded. Results showed that diagnostic reference levels (DRLs) in Ireland for barium meal examination was 17 Gy·cm² and barium enema examination was 47 Gy·cm².

Regarding the literature review, there are wide variations for same examination in different country depend on multifactor example exposure parameters, size of patients, equipment, examination procedure. Purpose of this study is to establish the local diagnostic reference levels for general radiography and fluoroscopy examinations with appropriate equipments and procedures in order to optimize patient protection at Ramathibodi Hospital.

CHAPTER IV

MATERIALS AND METHODS

4.1 Materials

4.1.1 Digital radiography machine

Digital radiography system model Philips Optimus and Digital Diagnost from the Department of Radiology, Faculty of Medicine, Ramathibodi Hospital were used in this study for patient dose measurements.



Figure 4.1 Digital radiography machine.

4.1.2 Digital fluoroscopy machine

Digital fluoroscopy system model Omni Diagnost, Philips from the Department of Radiology, Faculty of Medicine, Ramathibodi Hospital was used in this study for patient dose measurements.



Figure 4.2 Digital fluoroscopy machine.

4.1.3 Diagnostic Ion Chamber and kV Sensor Components

The X-ray tube output and half value layer were measured by a cylindrical ionization chamber type general purpose in beam chamber, (Rad/Cal corporation, model 10x6-6) serial number 01-1232 for digital diagnostic radiography system and digital fluoroscopy system. The chamber has active volume 6 cm^2 .

Accu kV diagnostic sensor (Rad/Cal corporation, model 40X12-W) serial number 52-0222 was used in this study for measurement dose, kV, mA and time in x-ray machine which was displayed by a microprocessor based control unit.

The Accu-Pro™ control unit (Rad/Cal corporation, model 9096) serial number 96-0164) was connected to various sensors to provide dose and X-ray beam information.



Figure 4.3 Accu-Pro™ Diagnostic Ion Chamber and kV Sensor Components

- A. Accu-Pro™ (9096) Control Unit
- B. 40x12-W Diagnostic Range kV Sensor
- C. 10X6-6 Ion Chamber Sensor
- D. Positioner
- E. 9660 Ion Chamber Digitizer
- F. 90C6-4 Sensor Cable

4.2 Methods

In this study, for general radiography examinations, the entrance surface air kerma were determined by X-ray tube output of digital radiography and exposure parameters information of each patient. Air kerma area products were recorded from KAP meter reading and exposure parameters information for each patient in fluoroscopy examination. The DRLs values from this study were compared with the diagnostic reference levels report by the National Radiological Protection Board, the International Atomic Energy Agency and the European Commission. Analysis of variance was performed to assess each result of study. Method consisted of 2 parts: general radiography and fluoroscopy (5).

The quality control (QC) tests of the machines were done in previously test by Department of medical sciences.

4.2.1 General radiography

The entrance surface air kerma was recommended by IAEA TRS 457 for the evaluation of patient dose and compare with other diagnostic reference levels value

in general radiography. Entrance surface air kerma from most common radiographic projections were evaluated as following; skull, anteroposterior/ posteroanterior and lateral, chest, posteroanterior, abdomen, anteroposterior, lumbar spine, anteroposterior and lateral.

The patients dose were evaluated in four steps. First, Half value layer was measured by ionization chamber in order to assess beam quality of X-ray tube. Then, the X-ray tube output was measured for each digital radiography systems in order to calculate incident air kerma value. Latter, the patient data was collected for each patient at least 10 patients per radiographic projection. According to <http://thailand.prd.go.th> (15), the average height in Thai men is 169.4 centimeters and 68.9 kilograms weight. The average height in Thai women is 156.9 centimeters and 57 kilograms weight. Therefore, a weight restriction criterion of 57 ± 5 kg for women and 69 ± 5 kg for men were applied for this study. Finally, the reference dose levels, mean, median and standard deviation of entrance surface air kerma were calculated for each radiographic projection.

A. Half value layer measurements.

Procedures for HVL measurement were as follows;

1. The X-ray equipments were set up for the select examination of a normal adult patient in the manual mode.
2. The ionization chamber was placed on the table which center was aligned with the X-ray beam.
3. Narrow beam geometry was performed in order to minimize the influence of scattered radiation.
4. The tube potential were selected at 60 kVp for X-ray room number six, 70, 73, 81 and 90 kVp for X-ray room number eight and 109 kVp for X-ray room number nine because of the most tube voltage were used for clinical examination of each X-ray room.
5. A tube loading 10 mAs was selected for measured half value layer because of the dosimeter readings are within the rated range of the instrument.
6. The detector was exposed and multiple exposures were performed to achieve higher accuracy.

7. Half value layer was recorded for each exposure and mean half value layer was calculated for multiple exposures.

B. X-ray tube output measurements

The output measurement was performed by methods as follows;

1. The focus to chamber distance 110 cm was performed which it used set up patient examination.
2. The ionization chamber position 50 cm above the patient support was placed in order to avoided backscatter radiation to active volume of ionization chamber which it center was aligned with the X-ray beam.
3. The exposure parameters were selected for each radiographic examination such as filtration, focus size, field size, tube voltage and tube loading.
4. The ionization chamber was exposed for three times and was recorded the dosimeter readings for each exposures.
5. The mean value of dosimeter readings was calculated.
6. The air kerma at the measurement point was calculated by equation 4.1

$$K(d) = \bar{M}N_{k,Q_0}k_Qk_{TP} \quad \dots \dots \dots 4.1$$

Where $K(d)$ is the air kerma at the measurement point(mR)
 \bar{M} is mean value of dosimeter readings (mR)
 N_{k,Q_0} is dosimeter calibration coefficient.
 k_Q is the correction factor for beam quality.
 k_{TP} is the correction factor for temperature and pressure.

7. The X-ray tube output was calculated by equation 4.2

$$Y(d) = \frac{K(d)}{P_{It}} \quad \dots \dots \dots 4.2$$

Where $Y(d)$ is the X-ray tube output at the measurement point(mR/mAs).
 $K(d)$ is the air kerma at the measurement point (mR).
 P_{It} is the tube loading during the exposure.

C. Patient data collection

Data collection of patients underwent common radiographic examination was performed as follows;

1. Clinical situations were set for the X-ray equipment, exposure parameters and position of the patient for the desire examination.
2. The patient thickness (t_p) at the center of the beam was measured after the patient was exposed.
3. Information on X-ray exposure parameters (tube voltage, tube loading) and geometric parameters (X-ray tube focus–film distance [FFD], X-ray tube focus–skin distance [FSD] and film size) were collected for each adult patient.

D. Entrance surface dose calculation

The inverse square law was used to calculate the incident air kerma from the X-ray tube output and exposure parameters for patient examinations. Entrance surface dose calculation of patients underwent common radiographic examination was performed as follows;

1. For each patient, the incident air kerma were calculated by equation 4.3 from the exposure parameters recorded on the worksheet such as tube voltage, tube loading, X-ray tube focus to patient support distance, distance of the X-ray tube output measurements and patient thickness.

$$K_i = Y(d)P_{It} \left(\frac{d}{d_{FTD} - t_p} \right)^2 \times 0.00876 \quad \dots \dots \dots 4.3$$

- Where
- Y(d) is the X-ray tube output measured at a distance d(cm) from the tube focus (mR/mAs).
 - P_{It} is the tube loading during the exposure of the patient.
 - d is the distance of the X-ray tube output measurements(cm).
 - d_{FTD} is the tube focus to patient support distance (cm).
 - t_p is the patient thickness(cm).
 - 0.00876 is the exposure to dose conversion factor (mGy/mR).

2. The entrance surface air kerma were calculated by equation 4.4. The measured HVL and the field size used during the examination were used for select appropriate backscatter factor for water from Appendix.

$$K_e = K_i B \quad \dots\dots\dots 4.4$$

Where K_i is the incident air kerma established for a given set of exposure parameters(mGy).

B is the backscatter factor of water for the selected field size.

3. The mean, median, third quartile values, minimum, maximum and standard deviation of the entrance surface air kerma were calculated for results from all patients in this study.

4.2.2 Fluoroscopy

The air kerma area product is dosimetric quantity that closely related to the energy imparted to the patient and to the effective dose. It was recommended for evaluate patient dose in fluoroscopy examination. Transmission ionization chamber or KAP meter was used for this quantity. It was evaluated in three steps. First, KAP meter was calibrated with reference dosimeter in clinical situation in order to calculated calibration coefficient of the reference dosimeter. Second, the patient data was collected for barium meal and barium enema examinations 50 patients per examination. Finally, the air kerma area product was calculated by KAP meter reading on console of fluoroscopy machine combined with calibration coefficient of the reference dosimeter.

A. Calibration of KAP meter.

The KAP meter was calibrated by methods as follows;

1. The calibrated diagnostic dosimeter position 20 cm above the patient support was placed and it center was aligned with the X-ray beam.

2. Field size 10 cm × 10 cm of the X-ray beam at the position of the chamber was performed.

3. The calibrated diagnostic dosimeter and the KAP meter were exposed for exposure parameter as following; tube voltage 50-120 kVp each step skip 10 kVp , tube loading 200 mA and time 10 msec.

4. The KAP meter ($M_{Q, KAP}$) reading and the reference chamber ($M_{Q, ref.}$) reading were recorded.

5. The calibrated diagnostic dosimeter was removed and was replaced by the image plate.

6. The image plate was exposed for exposure parameter as following; tube voltage 60 kVp, tube loading 200 mA and time 10 msec.

7. The nominal beam area (A) as the area contained within 50% of the maximum optical density was determined by a ruler.

8. The calibration coefficient, $N_{P_{KA}, Q}$ was calculated by equation 4.5.

$$N_{P_{KA}, Q} = \frac{M_Q^{ref}}{M_Q^{KAP}} N_{k, Q_0}^{ref} k_Q^{ref} A_{nom} \times 0.00876 \quad \dots \dots \dots 4.5$$

- Where
- $M_{Q, KAP}$ is reading of the KAP meter (μGym^2).
 - $M_{Q, ref}$ is reading of the calibrated diagnostic dosimeter (mR).
 - N_{k, Q_0}^{ref} is the calibration coefficient of the reference dosimeter obtained at a beam quality Q_0 .
 - k_Q^{ref} is the correction factor for difference of the chamber response between beam qualities Q_0 and Q .
 - A_{nom} is nominal beam area (m^2).
 - 0.00876 is exposure to dose conversion factor (mGy/mR).

B. Patient data collection.

Data collection of patients underwent barium meal and barium enema examinations were performed as follows;

1. The information of patients were recorded as following; age and sex.
2. The exposure parameters during the examinations were recorded as following; tube voltage, operating mode chosen, tube current, pulse rate, fluoroscopy time and KAP meter reading.

C. Calculation of air kerma area product.

Air kerma area product (P_{KA}) of patients underwent barium meal and barium enema examinations were calculated from the KAP meter reading by equation 4.6.

$$P_{KA} = MN_{P_{KA},Q_0} k_Q k_{TP} \dots \dots \dots 4.6$$

- Where k_{TP} is the correction factor for temperature and pressure.
- N_{P_{KA},Q_0} is the calibration coefficient in terms of the air kerma–area product for the radiation quality, Q_0 , used at the calibration temperature and pressure of T_0 and P_0 .
- T and P are temperature and pressure recorded during the measurement.
- k_Q is the correction factor for differences in the response of the KAP meter at the calibration quality, Q_0 , and at the quality, Q , of the clinical X-ray beam.

The mean, median, third quartile values, minimum, maximum and standard deviation of the air kerma–area product were calculated for results from all patients in this study.

CHAPTER V

RESULTS

In this chapter, the mean patient's characteristic and radiation dose recorded for patients referred for general radiography and fluoroscopy are shown and discussed. Furthermore, an assessment of the relationship between the radiation dose and the patients' weights, fluoroscopy time and number of images recorded was done using correlation coefficient (R) and coefficient of determination (R^2). The statistical significance of the linear relationships between the variables was ascertained by the probability value (p-value).

5.1 General radiography

The entrance surface air kerma was evaluated patient dose in general radiography. Half value layer and X-ray tube output were measured by ionization chamber in order to calculate entrance surface air kerma.

5.1.1 Half value layer measurements

Half value layer was measured by ionization chamber in order to assess beam quality of digital radiography and select backscatter factor for calculation entrance surface dose.

X-ray room no.6 was used for skull AP and lateral examination which used only 73 kVp tube voltage. The result showed HVL at 2.79 mmAl.

X-ray room no. 8 was used for KUB, lumbar spine AP and lumbar spine lateral examinations. The tube voltage was set in various values to match that on each examination and size of patient. The result is shown in table 5.1.

X-ray room no.9 was used for chest examination which used only 109 kVp tube voltage. The result showed HVL at 4.56 mmAl.

Table 5.1 The HVL of digital radiography in X-ray room no.8 for various tube voltages.

Tube voltage (kVp)	HVL (mmAl)
50	1.52
60	2.14
70	2.77
81	3.34
90	3.77
102	4.32

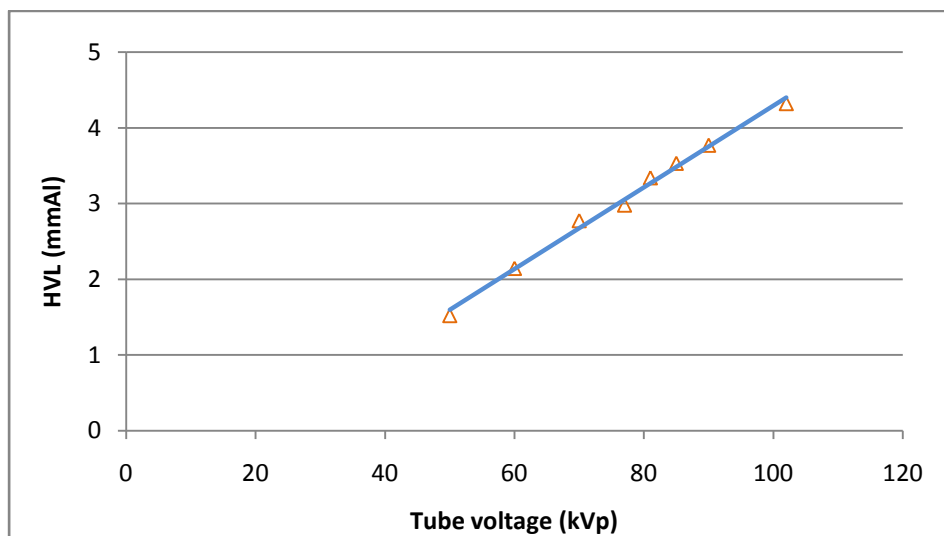
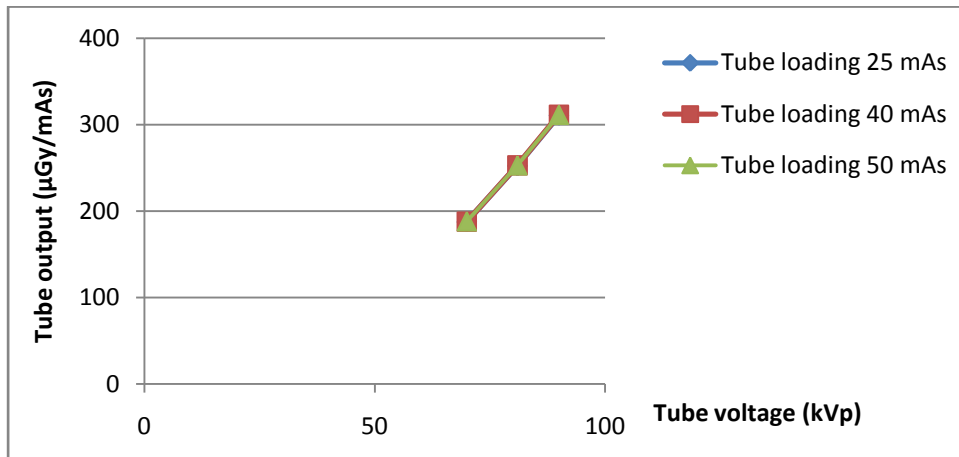


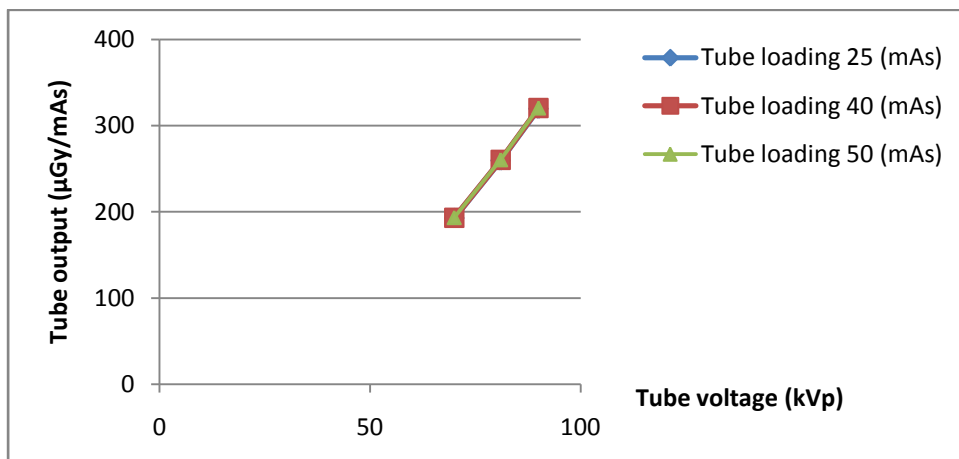
Figure 5.1 The HVL of various tube voltage for digital radiography in X-ray room no.8

5.1.2 X-ray tube output measurements

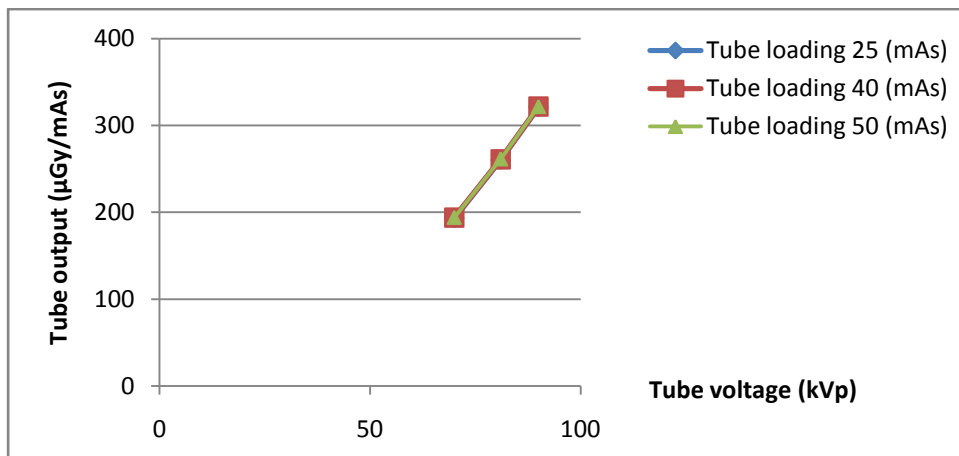
The tables 5.2 - 5.7 show the tube output of the digital radiography that was measured by varying the tube voltages, tube loadings and field size used in each patient.



A



B



C

Figure 5.2 The tube output as a function of various tube voltages and tube loadings for digital radiography in X-ray room no.8. (A) Field size 30 cm x 30 cm. (B) Field size 40 cm x 40 cm. (C) Field size 40 cm x 40 cm.

Table 5.2 The tube output of digital radiography in X-ray room no.6.

Tube voltage (kVp)	Tube loading (mAs)	Field size		Mean dosimeter reading (μGy)	Tube output ($\mu\text{Gy/mAs}$)
		X (cm)	Y (cm)		
73	20	22	30	4050.04	202.50
73	16	30	22	3271.86	204.49

Table 5.3. The tube output of digital radiography in X-ray room no.8 for field size 30 cm \times 30 cm.

Tube voltage (kVp)	Tube loading (mAs)	Mean dosimeter reading (μGy)	Tube output ($\mu\text{Gy/mAs}$)
70	25	4691.42	187.66
	40	7517.83	187.95
	50	9403.86	188.08
81	25	6308.51	252.34
	40	10113.42	252.84
	50	12645.06	252.90
90	25	7764.43	310.58
	40	12447.96	311.2
	50	15566.52	311.33

Table 5.4 The tube output of digital radiography in X-ray room no.8 for field size 40 cm × 40 cm.

Tube voltage (kVp)	Tube loading (mAs)	Mean dosimeter reading (μGy)	Tube output (μGy/mAs)
70	25	4813.62	192.55
	40	7723.25	193.08
	50	9662.28	193.25
81	25	6483.71	259.35
	40	10402.50	260.06
	50	13021.74	260.44
90	25	7985.18	319.41
	40	12807.12	320.18
	50	16030.80	320.62

Table 5.5 The tube output of digital radiography in X-ray room no.8 for field size 43 cm × 43 cm.

Tube voltage (kVp)	Tube loading (mAs)	Mean dosimeter reading (μGy)	Tube output (μGy/mAs)
70	25	4832.02	193.28
	40	7756.1	193.90
	50	9701.7	194.03
81	25	6513.5	260.54
	40	10437.54	260.94
	50	13074.30	261.49
90	25	8024.16	320.97
	40	12859.68	321.49
	50	16092.12	321.84

Table 5.6 The tube output of digital radiography in X-ray room no.9 for field size 35 cm × 35 cm.

Tube loading (mAs)	Mean dosimeter reading (μGy)	Tube output (μGy/mAs)
0.5	85.88	171.75
1	199.55	199.55
2	481.86	211.54
3.2	702.49	219.53
4	885.05	221.26
5	1115.15	223.03

Table 5.7 The tube output of digital radiography in X-ray room no.9 for field size 35 cm × 43 cm.

Tube loading (mAs)	Mean dosimeter reading (μGy)	Tube output (μGy/mAs)
0.5	85.88	171.75
1	199.55	199.55
2	481.86	240.93
3.2	702.49	219.529
4	885.05	221.26
5	1115.15	223.03

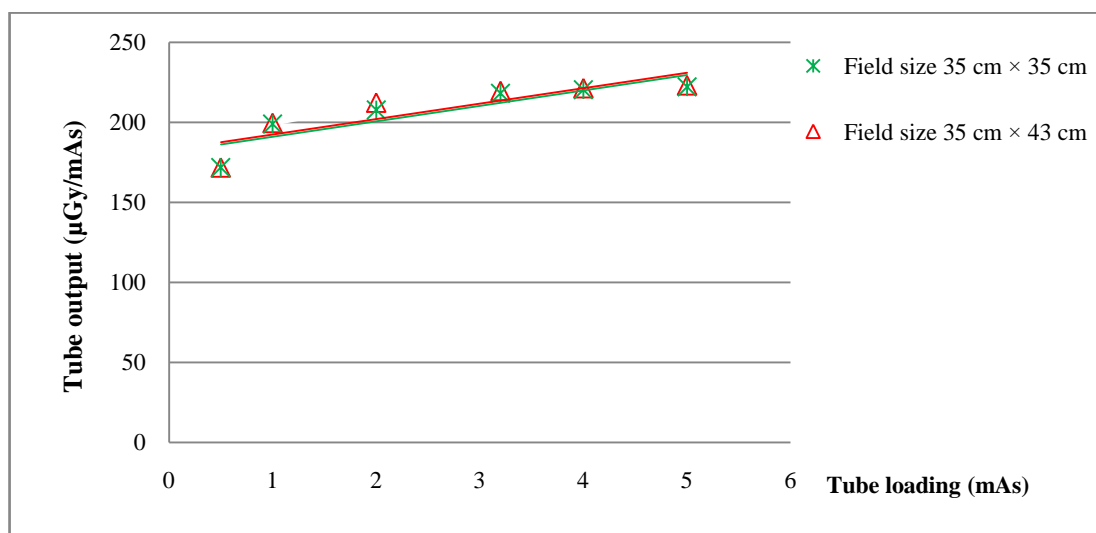


Figure 5.3 The tube output as a function of various tube loadings and 109 kVp tube voltage for digital radiography in X-ray room no.9.

5.1.3 Entrance surface air kerma

The patient dosimetry was determined in terms of the entrance surface air kerma (K_e) on the basis of X-ray tube output measurements and specific patient related exposure parameters using ionization chamber. Data were collected on Philips Optimus and Digital Diagnost digital radiographic systems. This study includes data from three digital radiography units in six digital radiographic examinations including skull AP, skull lateral, chest PA, abdomen AP, lumbar spine AP and lumbar spine lateral. A total of 180 patients (90 males and 90 females) were recruited to attend this study.

Table 5.8 shows the mean patient information and exposure parameters for six common radiographic examinations. Numbers of males and females were evenly divided. The mean, median, third quartile values, minimum, maximum, standard deviation, inter-quartile ranges and ratio of maximum/minimum of entrance surface air kerma were calculated for each examination as shown in table 5.9. The mean entrance surface air kerma for skull AP, skull lateral, chest PA, abdomen AP, lumbar spine AP and lumbar spine lateral were 1.70 ± 0.04 , 1.31 ± 0.02 , 0.05 ± 0.01 , 3.71 ± 0.48 , 5.56 ± 0.66 and 6.11 ± 0.55 mGy, respectively. Dose Reference Levels (DRLs) was determined by the third quartile value of entrance surface air kerma distribution for each examination.

We found that, the DRLs for skull AP, skull lateral, chest PA, abdomen AP, lumbar spine AP and lumbar spine lateral were 1.73, 1.33, 0.06, 4.05, 6.23 and 6.45 mGy, respectively.

Table 5.8 The mean patient information and exposure parameters for six common radiographic examinations.

Examinations	Patient thickness (mm)	Patient weight (kg)		Tube voltage (kV)	Tube loading (mAs)
		Male	Female		
Skull AP	193.91±10.54	67.4±5.6	56.7±6.63	73	20
Skull Lat.	172.04± 8.81	67.4±5.6	56.7±6.63	73	16
Chest PA	197.7±15.92	67.6±4.9	58.9±6.15	109	1.79±0.29
Abdomen AP	190.20±21.41	68.6±6.39	55.67±6.22	83.13±2.29	31.3±2.14
Lumbar spine AP	188.03±21.33	69.33±6.49	57.53±7.03	84.87±0.73	40
Lumbar spine Lat.	244.30±18.32	69.33±6.49	57.53±7.03	88.16±2.45	40.33±1.83

Table 5.9 The mean, median, third quartile values, minimum, maximum entrance surface air kerma in mGy, standard deviation, inter-quartile range and ratio of maximum/minimum for each examination.

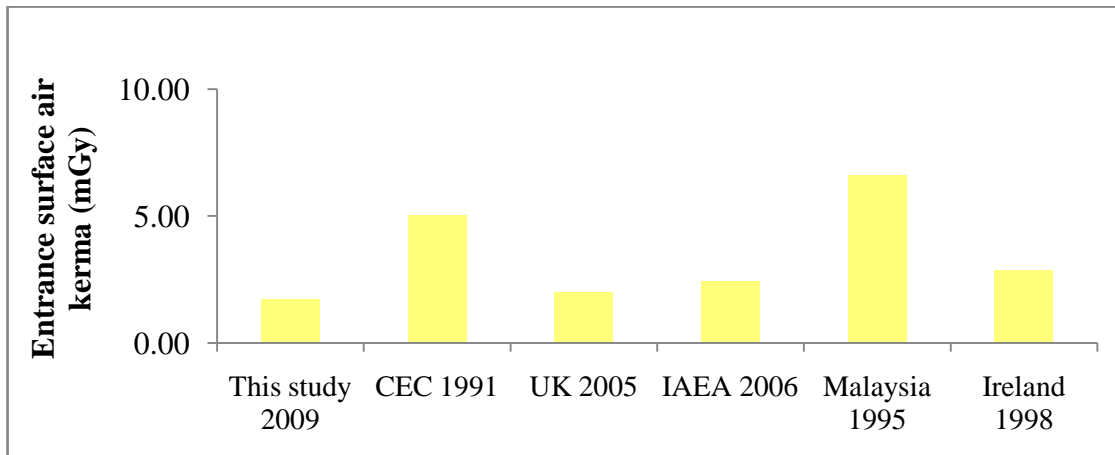
Examinations	Mean	Median	Third quartile	Min	Max	SD	Inter-quartile range	Ratio max/min
Skull AP	1.70	1.71	1.73	1.64	1.79	0.04	0.05	1.09
Skull Lat.	1.31	1.31	1.33	1.26	1.37	0.02	0.03	1.08
Chest PA	0.05	0.05	0.06	0.03	0.08	0.01	0.54	1.84
Abdomen AP	3.71	3.85	4.05	2.31	4.25	0.48	1.26	1.49
Lumbar spine AP	5.56	5.53	6.23	4.59	6.84	0.66	0.75	1.48
Lumbar spine Lat.	6.11	6.10	6.45	5.27	7.82	0.55	0.02	2.62

The standard deviation, inter-quartile range and ratios of maximum/minimum for each examination were shown variation of entrance surface air kerma for each patient. The standard deviations of entrance surface air kerma for individual patients were ranged from 0.01 for chest to 0.66 for lumbar spine AP. The inter-quartile ranges of entrance surface air kerma for individual patients were ranged from 0.02 for lumbar spine AP to 1.26 for abdomen AP. The ratios of maximum/minimum of entrance surface air kerma for individual patients were ranged from 1.08 for skull lateral to 2.62 for chest.

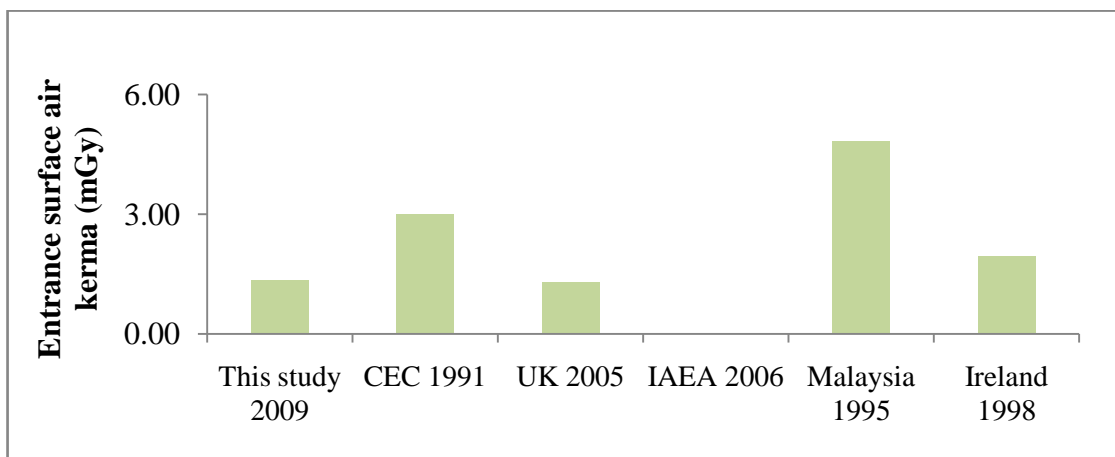
Table 5.10 presents the DRLs of this study compares with established DRLs from IAEA Basic safety standard 2006 (16), CEC 1991(17) and United Kingdom 2005 (18). The results showed the DRLs of this study was less than the value established by previous mentioned countries except skull lateral and lumbar spine AP examination. When compares the DRLs of this study with United Kingdom 2005, the percent difference for skull AP, skull lateral, chest PA ,abdomen AP, Lumbar spine AP and Lumbar spine lateral were -13.51, 2.32, -54.06, -3.64, 22.11 and -41.41 , respectively.

Table 5.10 A Comparison diagnostic reference levels of entrance surface air kerma in mGy for each examination.

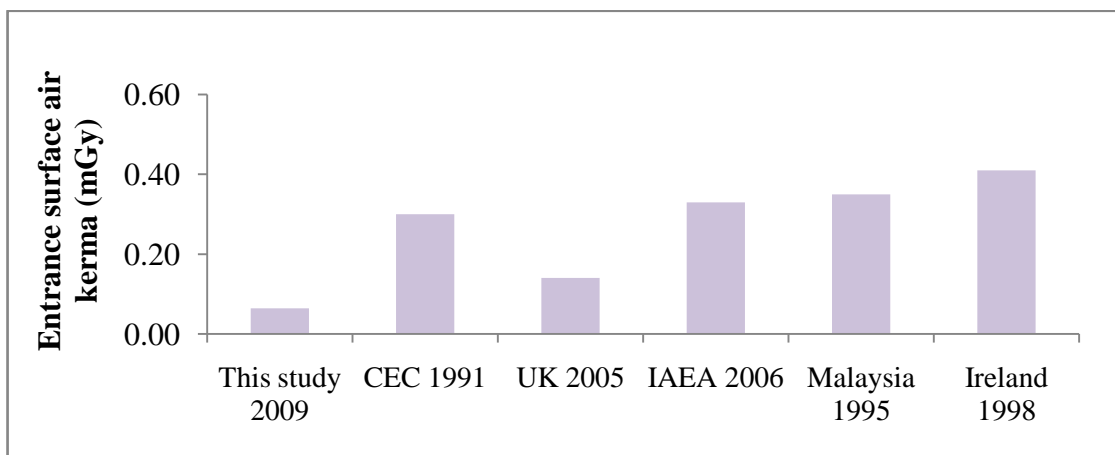
Examinations	This study 2009	CEC 1991 (16)		UK 2005 (18)		IAEA 2006 (16)		Malaysia 1995(10)		Ireland 1998 (11)	
		ESD	%diff	ESD	%diff	ESD	%diff	ESD	%diff	ESD	%diff
Skull PA	1.73	5.00	-65.40	2.00	-13.51	2.42	-28.52	6.85	-73.71	2.85	-39.3
Skull Lat.	1.33	3.00	-55.66	1.30	2.32	-	-	4.81	-72.35	1.93	-31.08
Chest	0.06	0.30	-78.56	0.14	-54.06	0.33	-80.51	0.35	-81.62	0.41	-84.31
Abdomen	4.05	10.00	-59.53	4.20	-3.64	3.64	11.18	13.82	-70.72	4.06	-0.32
L-S spine AP	6.23	10.00	-37.72	5.10	22.12	4.07	53.02	14.71	-57.66	3.43	81.57
L-S spine Lat.	6.45	30.00	-78.52	11.00	-41.41	8.53	-24.44	25.12	-74.34	8.41	-23.36



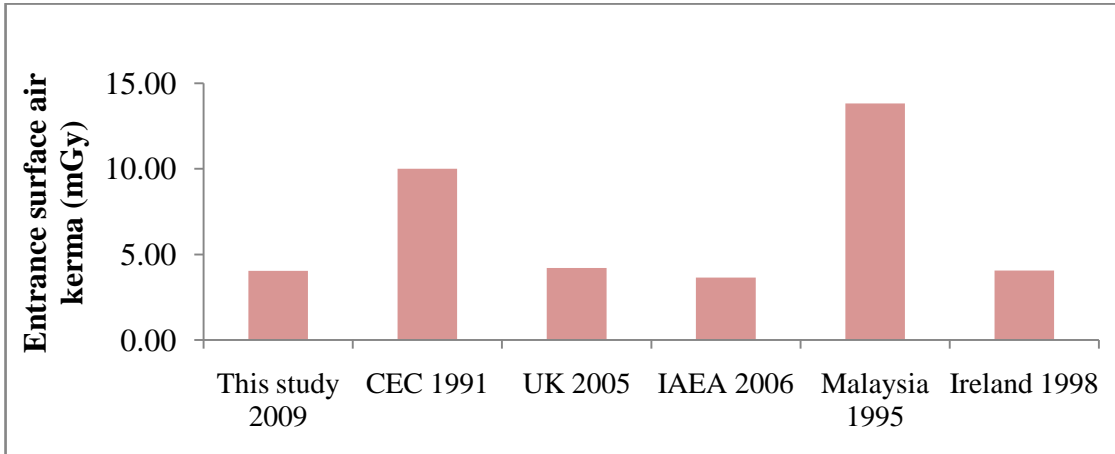
(A)



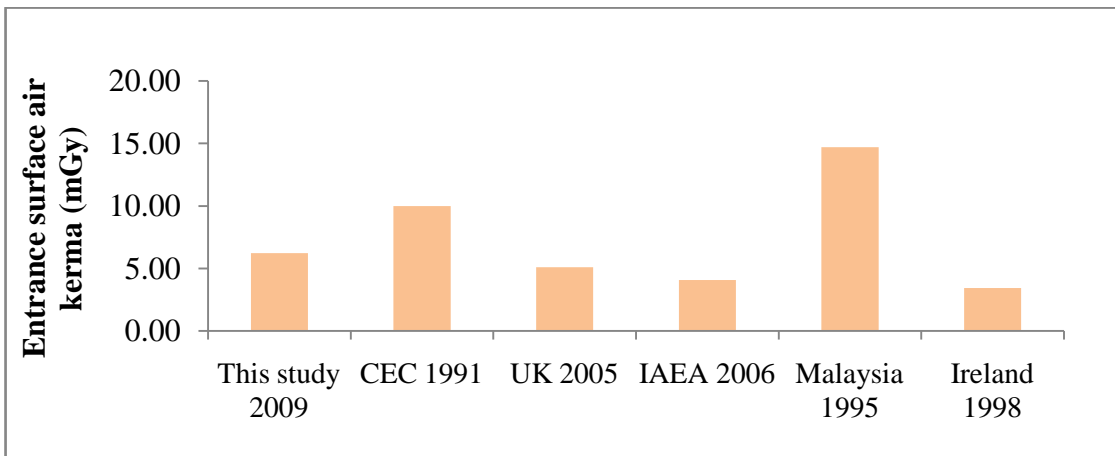
(B)



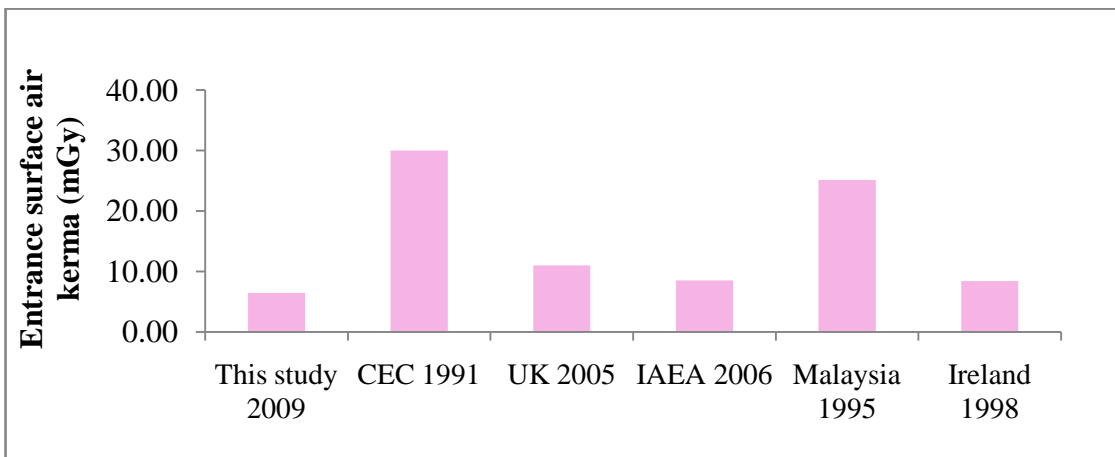
(C)



(D)



(E)



(F)

Figure 5.4 Comparison diagnostic reference level of entrance surface dose. (A). Skull AP. (B). Skull lateral (C). chest. PA (D). Abdomen AP (E). Lumbar spine AP (F). Lumbar spine lateral.

5.2 Fluoroscopy

The air kerma area was evaluated patient dose in fluoroscopy examination. Transmission ionization chamber or KAP meter was used for this quantity. Thus, calibration of KAP meter which build in fluoroscopy machine required to correct KAP meter reading on console of fluoroscopy machine.

5.2.1 KAP meter calibration

KAP meter was calibrated with reference dosimeter in order to calculate calibration coefficient for various tube voltage that use in clinical situation. The result is shown in table 5.11.

Table 5.11. The calibration coefficient of KAP meter in digital fluoroscopy.

Tube voltage (kVp)	Reference Dosimeter reading (mR)	Reference Dosimeter reading (μGy)	KAP meter reading (μGym^2)	Calibration coefficient
50	23.563	206.41	2.2	0.909914
60	38.68	338.84	3.6	0.912789
70	55.667	487.64	5.1	0.927281
80	75.08	657.7	6.9	0.924403
90	96.38	844.29	8.5	0.963284
100	119.7	1048.6	10.3	0.987287
110	144.83	1268.7	12.1	1.016879
120	171.53	1502.6	13.9	1.048383

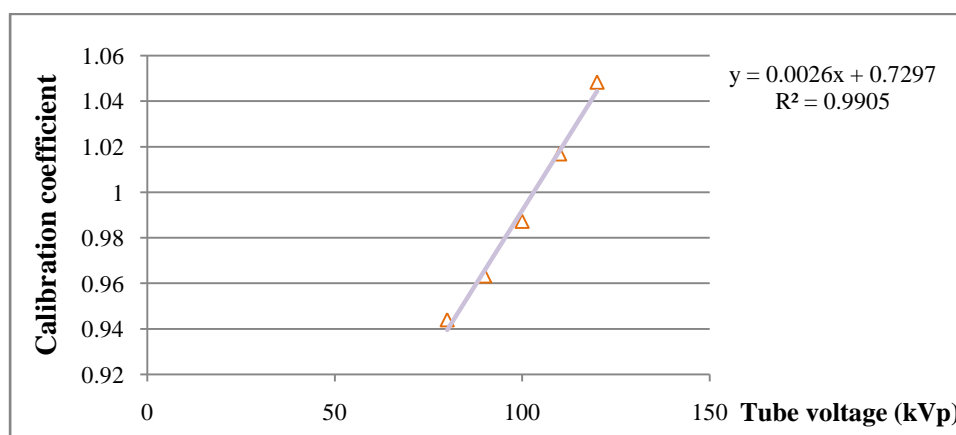


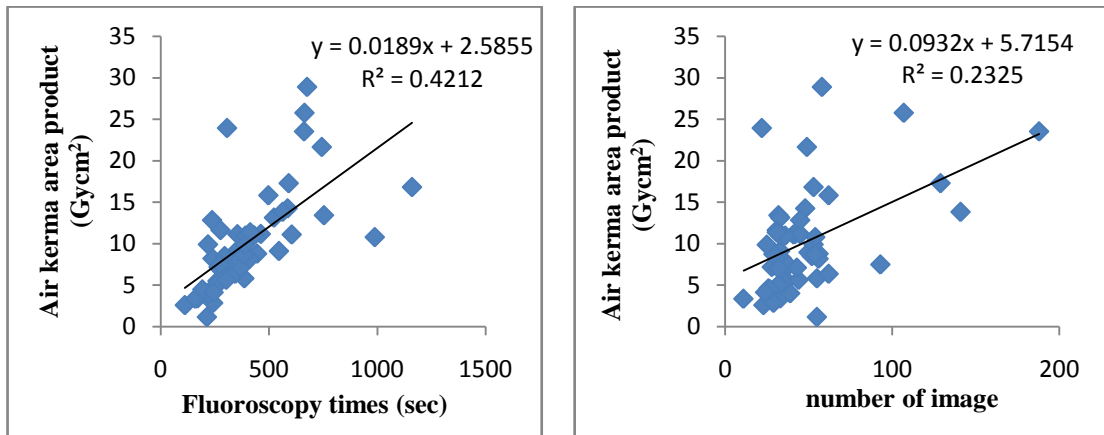
Figure 5.5 the calibration coefficient as a function of varies tube voltage for digital fluoroscopy.

5.2.2 Air kerma area product

The Air kerma area products (P_{KA}) in $Gy \cdot cm^2$ were calculated for barium meal and barium enema examinations. A total of 100 patients were observed in this study. The mean patient characteristic and exposure parameters for examinations can be found in table 5.12. The mean patient's age for barium meal was 61.5 ± 18.5 , and barium enema was 53.82 ± 14.52 .

For barium meal, the mean fluoroscopy time was 6.57 ± 3.59 seconds, and ranged from 110 to 1160 seconds. Figure 5.6 is a graph shown the correlation of the air kerma area products versus fluoroscopy time and air kerma area products versus number of image for barium meal examination. There were linear correlation between the Air kerma area products and fluoroscopy time were statistically significant (p-value < 0.05) as $R = 0.649$. The fluoroscopy time explaining 42.12% ($R^2 = 0.4212$) of the variation in the Air kerma area products values. The number of image for barium meal was 49.06 ± 31.94 which there are linear correlation with the Air kerma area products statistically significant (p-value < 0.05) as $R = 0.4822$. There were no images acquired in the radiographic mode. The number of images explaining 23.25% ($R^2 = 0.2325$) of the variation in the Air kerma area products values.

For barium enema, the mean fluoroscopy time was 6.44 ± 2.1 seconds, and ranged from 187 to 873 seconds. Figure 5.7 is a graph shown the correlation of the air kerma area products versus fluoroscopy time and air kerma area products versus number of image for barium enema examination. There were linear correlation between the Air kerma area products and fluoroscopy time were statistically significant (p-value < 0.05) as $R = 0.4305$. The fluoroscopy time explaining 18.53% ($R^2 = 0.1853$) of the variation in the Air kerma area products values. The number of image for barium enema was 16.28 ± 4.1 . There are linear correlation between the Air kerma area products and number of image statistically significant (p-value < 0.05) as $R = 0.4427$. The fluoroscopy time explaining 19.6% ($R^2 = 0.196$) of the variation in the Air kerma area products values. This study no images acquired in the radiographic mode.



01Figure 5.6 The correlation of the air kerma area products versus fluoroscopy time (left) and air kerma area products versus number of image (right) for barium meal examination.

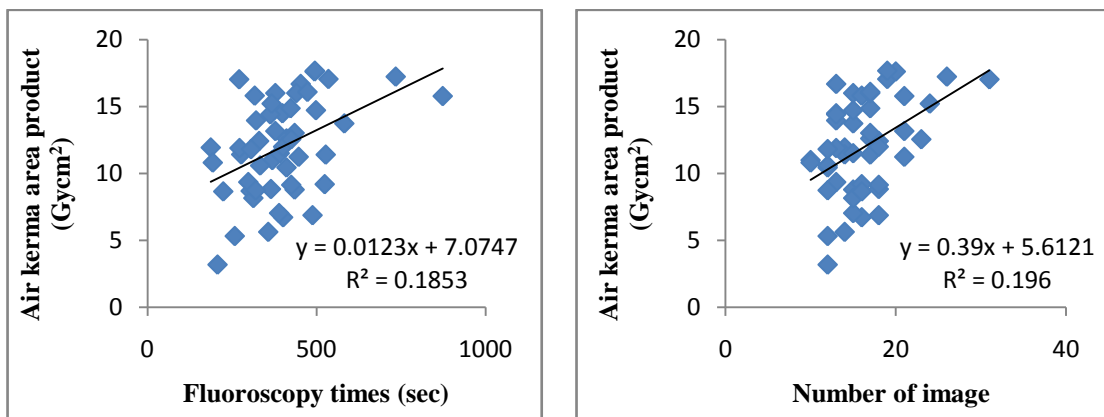


Figure 5.7 The correlation of the air kerma area products versus fluoroscopy time (left) and air kerma area products versus number of image (right) for barium enema examination.

Table 5.12 The mean patient characteristic and exposure parameters for barium meal and barium enema examinations.

Examinations	Patient age (years)	Tube potential (kV)	Fluoroscopy time (seconds)	No. of image per exam
Barium meal	61.5±18.5	84	406.64±211.49	49.06±31.94
Barium enema	53.82±14.52	96	396.36±125.05	16.28±4.1

Table 5.13 Air kerma area products in $\text{Gy}\cdot\text{cm}^2$ for barium meal and barium enema examinations.

Examinations	Mean	Median	Third quartile	Min	Max	SD	Inter-quartile range	Ratio max/min
Barium meal	10.29	8.87	12.53	1.17	28.87	6.17	6.57	24.65
Barium enema	11.96	11.91	14.82	3.19	17.66	3.58	5.66	5.53

The mean, median, third quartile values, minimum, maximum and standard deviation of air kerma area product were calculated for each examination as shown in table 5.13. The mean and diagnostic reference level for barium meal were 10.29 ± 6.17 and $12.53 \text{ Gy}\cdot\text{cm}^2$ and barium enema were 11.96 ± 3.58 and $14.82 \text{ Gy}\cdot\text{cm}^2$, respectively. Table 5.14 presents the DRLs of this study compares with established DRLs from Caroline (19), M Rio (20), Khatayut (21) and United Kingdom 2005. The results showed the DRLs of this study lower than the value established by other study except the value established by United Kingdom for barium meal this study higher than of 11.6 percent while barium enema was less than -39.01 percent.

Table 5.14 A Comparison diagnostic reference levels of Air kerma area product in $\text{Gy}\cdot\text{cm}^2$.

Research	Mean KAP ($\text{Gy}\cdot\text{cm}^2$)		DRLs KAP ($\text{Gy}\cdot\text{cm}^2$)		Fluoroscopy time (seconds)		Number of image	
	Barium meal	Barium enema	Barium meal	Barium enema	Barium meal	Barium enema	Barium meal	Barium enema
This study 2009	10.29	11.96	12.53	14.82	406	396	49.06	16.28
Caroline 2009	16.6	28.7	20.1	36.5	460	317	10	12
M Rio et al.	17	37	23	46	169	217	14.32	11.3
Khatayut 2007	18.2	40.8	-	-	372	236	-	-
UK 2005	-	-	11.2	24.3	103	122	22	12

CHAPTER VI

DISCUSSIONS

This study evaluated the radiation doses received by standard size of Thai population at Ramathibodi Hospital for general radiography and fluoroscopy examinations and establish diagnostic reference levels for these examinations. Additionally, the factors responsible for the variation in radiation doses were investigated and discussed in this chapter.

6.1 Entrance surface air kerma

Variation in mean patient thickness and exposure parameters found in abdomen AP examination was due to the fact that the manual mode was used for Ramathibodi hospital. The AEC mode was only used in chest examination. The comparison of DRLs of this study and CEC (1991), UK (2005), IAEA (2006), Malaysia (1995) and Ireland (1998) are presented in Table 5.10. The results showed that the DRLs for this study were less than the values established or surveyed by IAEA, CEC, UK, Malaysia and Ireland except skull lateral and lumbar spine AP examinations.

When compare with the UK data, we found that DRLs from this study were 3.64% to 54.06% less than the UK data surveyed in 2005 except, skull lateral and lumbar spine AP examinations, which our data showed 2.32% to 22.11% higher, respectively. This is mainly due to inappropriate in the exposure parameters; tube loading and field size for this study.

When compared our data with Ireland and Malaysia, which are in the health care level II countries as classified by the UNSCEAR. We found that the dose to patients from our data were generally less than those done in previously mentioned countries, except for the lumbar spine AP examination. This may be due to the differences in the radiography systems. Our newer data utilize the newer technology of

Digital Radiography. Compagnone et. al (22) compared radiation dose to patients undergoing standard radiographic examinations among conventional screen-film radiography, computed radiography and digital radiography. Their results showed that digital radiography used 29% to 43% lower radiation dose than those using screen film radiography or computed radiography, respectively.

Another Thai study done by Wichai et. al (23) , the entrance surface dose of patient undergoing chest radiography was measured at Srinagarind hospital. Their results showed that mean and third quartile values for digital chest radiography were 0.27 and 0.33 mGy, respectively. Warren-Forward HM and Millar JS (24) studied the optimization of radiographic technique for chest radiography. They found that increasing the tube potential from 60 kVp to 90 kVp would result in an entrance surface dose saving of 60 percent. When compare our data with another Thai data by Wichai et al, we found that the exposure parameters for chest examination of 109 kVp and 1.17-2.32 mAs for our study and 90 kVp, 3-14 mAs for their use. This confirms that increasing tube potential help decrease radiation dose to patient at similar population size.

The lower DRLs found in this study was a result from the differences in image receptor technology and exposure techniques used in digital radiography system. A CsI based a- Si TFT technology used in digital radiography has better detection efficiency than conventional screen-film system. With proper exposure parameters, one can optimize image quality while maintaining the lowest possible radiation dose exposed to the patients. The hospital DRL for lumbar spine AP examination for this study was higher than dose levels reported by other studies because the high tube potential, tube loading and wide field size was used. Further investigation should be carried out to optimize the dose and image quality, specific to the Thai patient population.

6.2 Air kerma area product

6.2.1 Barium meal

The DRL for barium meal from this study is $12.53 \text{ Gy}\cdot\text{cm}^2$ following the recommendation to set DRLs to the third quartile DAP value. This DRL is lower than the value established by Caroline is $20.1 \text{ Gy}\cdot\text{cm}^2$ and M Rio et al. is $23 \text{ Gy}\cdot\text{cm}^2$ except those obtained in the United Kingdom is $11.2 \text{ Gy}\cdot\text{cm}^2$ as shown in table 5.14. The mean DAP value of $10.29 \text{ Gy}\cdot\text{cm}^2$ recorded in this study was lower than those recorded in Khatayut study is $18.2 \text{ Gy}\cdot\text{cm}^2$ as shown in table 5.14. Khatayut study had been evaluated the radiation doses received by patients during barium meal and barium enema examinations for conventional fluoroscopy in 4 hospitals located in udonthani province.

6.2.2 Barium enema

The DRL for barium enema from this study is $14.82 \text{ Gy}\cdot\text{cm}^2$. This DRL is lower than the value established by Caroline is $36.5 \text{ Gy}\cdot\text{cm}^2$, M Rio et al. is $46 \text{ Gy}\cdot\text{cm}^2$ and the United Kingdom is $24.3 \text{ Gy}\cdot\text{cm}^2$ as shown in table 5.14. The mean DAP value of $11.96 \text{ Gy}\cdot\text{cm}^2$ recorded in this study was lower than those recorded in Khatayut study is $40.8 \text{ Gy}\cdot\text{cm}^2$ as shown in table 5.14.

6.2.3 Fluoroscopy time

In this study, the mean fluoroscopy time for barium meal and barium enema examinations were 406 seconds and 396 seconds, respectively. These means fluoroscopy times are longer than the time recorded by Caroline, M Rio et al. and the United Kingdom. The long fluoroscopy time may be affected by co-operation of patient, pathology and radiologist. Radiologists are capable of controlling the fluoroscopy time by modifying the technique used for barium meal and barium enema examinations.

6.2.4 Number of images

The mean number of images for barium meal was 49.06 ± 31.94 and barium enema was 16.28 ± 4.1 . There were no images acquired in the radiographic mode.

These means number of images are more than the images acquired by Caroline, M Rio et al. and the United Kingdom. Caroline had been studied radiation doses for barium meals and barium enemas examination at 3 hospitals in the Western Cape South Africa and the digital fluoroscopy unit used in 2 hospitals.

The digital radiography technology in this study offered low radiation dose to patient but most the number of radiograph images and the long fluoroscopy time influence radiation dose to patient. Therefore reduction the radiation dose in patient could be succeeded by taking few numbers of radiograph image and shorter fluoroscopy time.

CHAPTER VI

CONCLUSIONS

The DRLs for common radiographic examinations for Thai patients undergoing digital radiographic examination were established in local level. The hospital should establish the DRLs that are appropriate to their equipment, exposure parameter, examination procedure and patient size in order to optimize patient dose. The DRLs value should be reviewed at appropriate intervals, adapted to new exposure parameter, examination procedure and equipment. The examination has DRL value above reference organization, should be investigated and either justify high dose or review exposure parameter, examination procedure and equipment to reduce patient dose.

This study was though performed in a standard size Thai patient on the basis of X-ray tube output measurements and specific patient related exposure parameters using ionization chamber. A future study in children should be carried out to ensure the patient doses are as low as reasonably achievable. Owing to the detriment for same effective dose in children are generally greater than adults. Therefore the stochastic radiation risks of carcinogenesis and genetic effects are generally greater for children than for adults.

REFERENCES

1. Bushberg T Jerrold, J. Anthony Seibert, Edwin M. Leidholdt Jr, John M. Boone. Essential Physics of Medical Imaging (2nd Edition). 2nd ed. USA: Lippincott Williams & Wilkins; 2002
2. Chotas HG, Dobbins JT 3rd, Ravin CE. Principles of Digital Radiography with Large-Area, Electronically Readable Detectors: A Review of the Basics. Radiology. 1999; 210(3):595-599.
3. Hirshfeld JW Jr, Balter S, Brinker JA, Kern MJ, Klein LW, Lindsay BD, et al. ACCF/AHA/HRS/SCAI clinical competence statement on physician knowledge to optimize patient safety and image quality in fluoroscopically guided invasive cardiovascular procedures. Circulation. 2005;111(4):511-32.
4. HART D, Hillier MC, Wall BF. National reference doses for common radiographic, fluoroscopic and dental X-ray examinations in the UK. Br J Radiol. 2009; 82(973):1-12.
5. International Atomic Energy Agency. Dosimetry in diagnostic radiology: an international code of practice. Technical reports series no. 457. Vienna: International Atomic Energy Agency; 2007
6. The international commission on radiological protection. ICRP report 92: Relative biological effectiveness (RBE), quality factor (Q), and radiation weighting factor(WR). Bethesda, Maryland, USA: ICRU; 2003
7. International Commission on Radiation Units and Measurements. ICRU Report 74 : Patient dosimetry for X ray used in medical imaging. Bethesda Maryland USA: ICRU; 2006.
8. The international commission on radiological protection. ICRP report 103: The 2007 Recommendations of the International Commission on Radiological Protection. ICRP Publication 103. Ann. ICRP 37 (2-4).

9. The Emergency Care Research Institute (ECRI) and The Institute for Safe Medication Practices (ISMP). Diagnostic ionizing radiation and pregnancy: Is there a concern?. Pennsylvania Patient Safety Advisory. 2008; 5(1):3-15.
10. Ng KH, Rassiah P, Wang HB, Hambali AS, Muthuvellu P, Lee HP. Doses to patients in routine X-ray examinations in Malaysia. Br J Radiol. 1998; 71(846):654-660.
11. Johnston DA, Brennan PC. Reference dose levels for patients undergoing common diagnostic X-ray examinations in Irish hospitals. Br J Radiol. 2000; 73(868):396-402.
12. Schuncke A, Neitzel U. Retrospective patient dose analysis of a digital radiography system in routine clinical use. Radiat Prot Dosimetry. 2005;114(1-3):131-4.
13. Kim YH, Choi JH, Kim CK, Kim JM, Kim SS, Oh YW, et al. Patient dose measurements in diagnostic radiology procedures in Korea. Radiat Prot Dosimetry. 2007; 123(4):540-545.
14. Carroll EM, Brennan PC. Radiation doses for barium enema and barium meal examinations in Ireland: potential diagnostic reference levels. Br J Radiol. 2003; 76(906):393-397.
15. The Government Public Relations Department [Internet]. Thailand: 2009 [updated 2009 Mar 13; cited 2012 May 02]. PRD Office of the Prime Minister; Available from: http://thailand.prd.go.th/view_news.php?id=4123&a=2.
16. Muhogora WE, Ahmed NA, Almosabihi A, Alsuwaidi JS, Beganovic A, Ciraj-Bjelac O, et al. Patient doses in radiographic examinations in 12 countries in Asia, Africa, and Eastern Europe: initial results from IAEA Projects. AJR Am J Roentgenol. 2008; 190(6):1453-61
17. European Commission. Radiation protection 109. Guidance on diagnostic reference levels (DRLs) for medical exposures, Radiat Prot. 1999
18. HART D, HILLIER MC, WALL BF. National reference doses for common radiographic, fluoroscopic and dental X-ray examinations in the UK. Br J Radiol. 2009; 82(973):1-12.

19. Nabasenja C. Radiation doses for barium meals and barium enemas in the Western Cape South Africa (Thesis). Cape Town, Cape Peninsula University of Technology; 2009. 122p.
20. Río M, Pérez S, Herreros A, Coll A, Ruiz A, Baró J et al. Reference value assessment for DAP measured with a transmission ion chamber in gastrointestinal tract examinations. Spanish Radiation Protection Society.
21. Nigaprake K. Radiation dose for barium enema and barium meal examinations in Udonthani. Bull Dept Med Sci. 2007; 49(1): 19-43.
22. Compagnone G , Baleni MC, Pagan L, Calzolaio FL, Barozzi L, Bergamini C. Comparison of radiation doses to patients undergoing standard radiographic examinations with conventional screen-film radiography, computed radiography and direct digital radiography. Br J Radiol. 2006; 79(947):899-904.
23. Witchathorntrakun W, Wongsanon S and Kheonkaew B. Skin radiation dose of patient undergoing chest radiography in Srinagarind Hospital, Faculty of Medicine, Khon Kaen University Srinagarind Medical Journal. 2010; 25(2):120-124.
24. Warren-Forward HM and Millar JS. Optimization of radiographic technique for chest radiography. Br J Radiol. 1995; 68(815):1221-1229.

APPENDIX

Backscatter factor for general radiography and fluoroscopy

The backscatter factor, B was introduced in chapter 4. It is the conversion coefficient that relates the incident air kerma to the entrance surface air kerma thus :

$$K_e = K_i B$$

The backscatter factors were calculated by Petoussi-Henss et al. for homogeneous phantoms. These data were selected because they have been calculated in terms of air kerma, which they cover the necessary range of field sizes and diagnostic spectra. They are available for three backscatter materials. In addition, the data have been successfully validated by comparison with the results of Harrison, Bartlett et al. and Grosswendt.

Table A-1 gives the values of the Petoussi-Henss et al. backscatter factors for field sizes of 100 mm × 100 mm, 200 mm × 200 mm and 250 mm × 250 mm, 21 X ray spectra with X-ray tube voltages between 50 kV and 150 kV and for backscattering materials, including water and ICRU tissue of density 1.00 g/cm³ (elemental composition 10.1% H, 11.1% C, 2.6% N and 76.2% O). The data for PMMA are included as they may be of value when dosimeters are calibrated with PMMA backscatter present. All the data in the table were calculated at a focus to skin distance of 1000 mm and with a scattering slab of entrance area 300 mm × 300 mm and thickness 150 mm. This thickness provides full backscatter. The data in the table are for three different tube filtrations (2.5 mm Al, 3.0 mm Al and 3.0 mm Al + 0.1 mm Cu). Values of the backscatter factor at HVLs between the tabulated points may be obtained by linear interpolation. Data for square fields of areas between 100 mm × 100 mm and 250 mm × 250 mm may also be obtained by linear interpolation. Above the latter field size, the backscatter factor may be assumed to be constant with sufficient accuracy (the largest difference in Table A-1 between the backscatter factors for the 200 mm × 200 mm and the 250 mm × 250 mm data is less than 2%). It is suggested that backscatter factors for rectangular fields (of length L and width W) be obtained for the 'equivalent square' field of side L_{equiv} given by

$$L_{equiv} = \frac{2LW}{(L + W)}$$

It should be noted that there are important differences between the backscatter factors for the three materials in the table. The differences vary with field

size and X-ray spectrum and are the greatest between water and PMMA where they can be as large as 9%. The backscatter factors in the table range between 1.24 and 1.67.

Table A-1. The backscatter factor for water, ICRU tissue and PMMA for 21 diagnostic x ray beam qualities and for three field sizes at a focus to skin distance of 1000 mm.

Tube voltage (kV)	Filter	Backscatter factor (B)									
		Field size	100mm x 100 mm			200mm x 200 mm			250mm x 250 mm		
		HVL	Water	ICRU	PMMA	Water	ICRU	PMMA	Water	ICRU	PMMA
		(mm Al)	tissue			tissue			tissue		
50	2.5 mm Al	1.74	1.24	1.25	1.33	1.26	1.27	1.36	1.26	1.28	1.36
60	2.5 mm Al	2.08	1.28	1.28	1.36	1.31	1.32	1.41	1.31	1.32	1.42
70	2.5 mm Al	2.41	1.30	1.31	1.39	1.34	1.36	1.45	1.35	1.36	1.46
70	3.0 mm Al	2.64	1.32	1.32	1.40	1.36	1.37	1.47	1.36	1.38	1.48
70	3.0 mm Al										
	+0.1 mm Cu	3.96	1.38	1.39	1.48	1.45	1.47	1.58	1.46	1.47	1.59
80	2.5 mm Al	2.78	1.32	1.33	1.41	1.37	1.39	1.48	1.38	1.39	1.50
80	3.0 mm Al	3.04	1.34	1.34	1.42	1.39	1.40	1.51	1.40	1.41	1.52
80	3.0 mm Al										
	+0.1 mm Cu	4.55	1.40	1.40	1.49	1.48	1.50	1.61	1.49	1.51	1.63
90	2.5 mm Al	3.17	1.34	1.34	1.43	1.40	1.41	1.51	1.41	1.42	1.53
90	3.0 mm Al	3.45	1.35	1.36	1.44	1.42	1.43	1.53	1.42	1.44	1.55
90	3.0 mm Al										
	+0.1 mm Cu	5.12	1.41	1.41	1.50	1.50	1.51	1.62	1.51	1.53	1.65
100	2.5 mm Al	3.24	1.34	1.34	1.42	1.40	1.41	1.51	1.41	1.42	1.53
100	3.0 mm Al	3.88	1.36	1.37	1.45	1.44	1.45	1.55	1.45	1.46	1.57
100	3.0 mm Al										
	+0.1 mm Cu	5.65	1.41	1.42	1.50	1.51	1.53	1.64	1.53	1.55	1.66
120	3.0 mm Al	4.73	1.37	1.38	1.46	1.46	1.48	1.58	1.48	1.49	1.60

Table A-1. The backscatter factor for water, ICRU tissue and PMMA for 21 diagnostic x ray beam qualities and for three field sizes at a focus to skin distance of 1000 mm (cont.).

Tube voltage (kV)	Filter	Backscatter factor (B)									
		Field size	100mm x 100 mm			200mm x 200 mm			250mm x 250 mm		
		HVL	Water	ICRU	PMMA	Water	ICRU	PMMA	Water	ICRU	PMMA
		(mm Al)	tissue			tissue			tissue		
120	3.0 mm Al										
	+0.1 mm Cu	6.62	1.41	1.42	1.50	1.53	1.54	1.64	1.54	1.56	1.67
130	2.5 mm Al	4.32	1.36	1.36	1.44	1.44	1.45	1.55	1.45	1.47	1.57
150	2.5 mm Al	4.79	1.36	1.36	1.44	1.45	1.46	1.55	1.46	1.48	1.58
150	3.0 mm Al	6.80	1.39	1.39	1.47	1.50	1.51	1.61	1.52	1.53	1.63
150	3.0 mm Al										
	+0.1 mm Cu	8.50	1.40	1.41	1.48	1.53	1.54	1.64	1.55	1.57	1.67

BIOGRAPHY

NAME	Kronvadee Promsupap
DATE OF BIRTH	14 April 1983
PLACE OF BIRTH	Nakhonratchasima, Thailand
INSTITUTIONS ATTENDED	Mahidol university, 2004 Bachelor of Science (Radiological Technology) Mahidol university, 2011 Master of Science (Medical Physics)
HOME ADDRESS	307/1 Moo 5, Tambon Buengpali, Amphoe kaengsanamng, Nakhonratchasima, 30440 Tel. 083-9249349 E-mail : koirt37@hotmail.com